A 700-year record of climate and environmental change from a high Andean lake: Laguna del Maule, central Chile (36°S)

María L Carrevedo[1,2,3], Matías Frugone[3,4], Claudio Latorre[1,2,3,5], Antonio Maldonado[6,7], Patricia Bernárdez[8], Ricardo Prego[9], Daniela Cárdenas[6] and Blas Valero-Garcés[3,4]

[1]Departamento de Ecología, Pontificia Universidad Católica de Chile, Chile

[2]Institute of Ecology and Biodiversity (IEB), Santiago, Chile

[3]Laboratorio Internacional de Cambio Global (LINCGlobal), PUC-CSIC, Chile-Spain

[4]Pyrenean Institute of Ecology, Consejo Superior de Investigaciones Científicas, IPE-CSIC, Spain

[5]Nucleo Milenio de Paleoclima del Hemisferio Sur, Santiago, Chile

[6]Centro de Estudios Avanzados en Zonas Áridas (CEAZA), Universidad de La Serena, Chile

[7]Universidad Católica del Norte, Chile

[8] Universidad de Vigo, Spain

[9] Instituto de Investigaciones Marinas (IIM-CSIC), Spain

Corresponding author:

María L Carrevedo, Departamento de Ecología, Pontificia Universidad Católica de Chile, Alameda 340, Santiago, Chile, CP 6513677. Tel.: + 56-2- 354-2822; fax: + 56-2-354 2621. E-mail: mcarrevedo@bio.puc.cl

Abstract

Central Chile is heavily exploited for mineral and water resources, with agriculture and large urban populations all creating intensive landscape use. Few records of past environmental and climate change are available that afford a broader context. To aid in this assessment, we present a 700 yr reconstruction from Laguna del Maule (LdM) in the high Andes of central Chile based on sedimentological, geochemical, diatom and pollen analyses. The age model is based on $^{210}Pb/^{137}Cs$ and ^{14}C dating tied into known volcanic eruptions. Sedimentology consists of organic-rich sediments and diatom oozes with several interspersed volcanic-rich facies and two tephra deposits. Sediment geochemistry exhibits increased productivity (high Br/Ti, biosilica) and more dominant oxic conditions (high Fe/Mn) from 1300–1400 AD and from 1650–1850 AD, likely during periods of relatively lower lake levels and better development of littoral environments. However, during this later period, high elevation vegetation was dominant, indicative of regional cooler/wetter conditions. In contrast, sediments deposited from 1850-1930 AD evidence decreased productivity and increased anoxic lake bottom conditions. The LIA in LdM is characterized by significant variations in lake dynamics and hydrology with cooler/wetter conditions (1570-1700 AD), major environmental changes in the 18th century and ending at ca 1850 AD. LdM record documents the impact of the LIA in the southern hemisphere and stresses

the global nature of this climate period. Large changes in lake dynamics and diatoms assemblages during the 20th century could be related to anthropogenic impacts but recent changes in climate patterns cannot be excluded.

Keywords

Diatoms, geochemistry, pollen, Little Ice Age, Chile, Late Holocene

1. Introduction

Anthropogenic activities have resulted in significant and profound impacts on the Earth's climate, ecosystems and biogeochemical cycles since late 18th century (e.g., IPCC AR4, 2007; AR5, 2014; Rodhe et al., 1995; Smol, 2008). In the light of increasing greenhouse gas emissions, global warming, human impact and land cover changes, Crutzen and Stoermer (2000) coined the term "Anthropocene" for this most recent period of the Earth's history. Yet, it is often in the context of long-term regional changes including natural drivers of variability that such impacts can truly be assessed.

Despite significant progress in late Quaternary research across Chile (i.e. Latorre et al., 2007), and recent interannual and multi-decadal reconstructions of temperature

variations for South America for the past millenium (Neukom et al., 2011); there is less information regarding past climate change and long-term dynamics of central Chile ecosystems. Tree-rings (Christie et al., 2010; Le Quesne et al., 2006) and lake records (Boes and Fagel, 2008; De Jong et al., 2013; Fagel et al., 2010; Jenny et al., 2002a, b, 2003; Urrutia et al. 2010; Von Gunten et al., 2009a,c; Moy et al., 2008 Chambers et al., 2014; Moreno et al., 2014) provided late Holocene reconstructions of climate and human impact. These records have demonstrated significant changes during the last millennium, some synchronous to the Little Ice Age (LIA, i.e., 1570-1900 AD, see Matthews and Briffa, 2005) and the Medieval Climate Anomaly (MCA 500- 1350 AD, Graham et al., 2007) although the regional timing of these fluctuations often show discrepancies in duration and intensity. Available records demonstrate a significant human impact in mountain ecosystems over the past few centuries. Copper mining and associated land use have had a strong effect through airborne pollutants and eutrophication in central Chile Andean lakes (Von Gunten et al., 2009a). Other high elevation lakes in central Chile (i.e., lakes Chepical and Laja) also exhibit large environmental fluctuations in the 20th century, yet the impact of human activities in explaining such trends has not been evaluated.

To aid in this assessment, a 700 year high-resolution reconstruction of past climate and environmental variability was developed based on limnological variations of Laguna

del Maule (LdM), a volcanic lake situated in the high Andes of central Chile (Figure 1a, b). For this, a combination of sedimentological, geochemical and biological proxies was used together with an age model based on multiple dating methods. This multiproxy approach is well suited for addressing the challenges of reconstructing past environmental conditions from lake sequences in the high Andes, as various components of lake systems are mediated by non-climatic factors, such as geomorphology, volcanism, local hydrology, the magnitude of response to climatic forcing for any given lake system may be non-linear (Fritz, 2008). In this paper, the timing of major environmental changes at LdM is established along with how these relate to regional and global climate change (such as the onset and demise of the LIA) and human and climate synergies of 20th century changes in Andean high altitude lakes.

[insert Figure 1]

2. Site description

LdM (36°S-70°W, 2160 masl) is located in a large caldera in the western (windward) central Chilean Andes. The LdM volcanic field, located in the Andean Southern Volcanic Zone, extends over 500 km^2 and comprises more than 130 individual vents (Figure 1a, b). Past eruptive history (Hildreth et al., 2010) includes silicic eruptions, generating welded ignimbrites associated with caldera formation, small rhyolitic eruptions,

111 and a culminating ring of 36 post-glacial (< 25 ka) rhyodacite and rhyolite coulees and
112 domes that encircle the lake (Feigl et al., 2014). Using satellite radar interferometry,
113 Fournier et al. (2010) measured a deformation field rate of ~180 mm/year between 2007
114 and 2008, which continues until the present.
115 LdM is located in the transition zone between the temperate, semi-arid, summer
116 warm (Csb) and the dry-cool high-mountain (E) climate (Koppen-Geiger classification).
117 Median annual temperatures recorded from 2007 to 2013 are: 8.4, 9.6, 10.3, 9.5, 8.1, 9.1
118 and 9.1 °C respectively; whereas for 2014 data was available only until September 23 with
119 7.6°C. The coldest temperature registered was -8 °C (August 2013). Precipitation stemming
120 off cold fronts originates in the mid-latitudes and is most prevalent in autumn (May) to
121 winter months (August) (Garreaud, 2009). Occasional summer storms can also occur when
122 favorable conditions aloft allow the advection of moist air masses from the east (Viale and
123 Garreaud, 2014). On interannual to interdecadal timescales, rainfall in subtropical central
124 Chile has been shown to be sensitive to variations in the El Niño-Southern Oscillation
125 (ENSO), the Southern Annular Mode (SAM) and the Pacific Decadal Oscillation (PDO)
126 (Garreaud, 2009; Montecinos et al., 2011; Quintana and Aceituno, 2012). Recent decades
127 of global warming (Trenberth and Fasullo, 2013) and projected future changes in the

128 subtropics worldwide (IPCC AR5, 2014) indicate that areas such as central Chile could
129 become drier as winter droughts increase in frequency.
130 Modern vegetation surrounding LdM is dominated by sub-shrubs and cushion
131 species and is part of high Andean Shrubland belt (between 2000-2500 masl) (García
132 Berguecio, 2006; Luebert and Pliscoff, 2006; Teillier et al., 2011). At higher elevations,
133 high Andean Steppe (>2500 masl) is dominated by herbs and cushion species characterized
134 by scattered and/or scarce vegetation. Low Andean Shrublands occur at elevations between
135 1500-2000 masl and Deciduous Forest is found at elevations lower than 1500 m (see Table
136 2 in Supplemental Files).
137 LdM is a 54 km² lake with a maximum depth of 50 m, part of the Maule river
138 watershed (21075 km^2). The lake is irregularly shaped (Figure 1c) and was dammed
139 (construction from 1946-1958, Figures 2, 3, 4, 5, 6, 7e-g). The dam is 40 m higher than the
140 former lake level and the maximum potentially flooded area is 56 km^2 (Sandoval Jeria,
141 2003). As a consequence, the lake volume increased from ~6 x 10^8 m^3 to more than 2 x10^9
142 m^3 (Arias, 2011). Lake level fluctuations in recent decades have responded mostly to
143 reservoir management for irrigation and hydroelectric needs. Indeed, the lake level has
144 experienced a severe drop of 27 m in the last seven years (see Figures 1, 2, 3 in
145 Supplemental Files). LdM is fed by winter snow accumulation (minimum of 0.01m in May,

146 2010 to a maximum of 3.8 m in September, 2014, see Figure 3 in Supplemental Files) and
147 spring snowmelt. Although limnological data are scarce, depth, local climate and basin
148 geomorphology all possibly indicate that the mixing pattern of LdM corresponds to a
149 dimictic lake. The lake often freezes over in winter at the sectors of Las Nieblas, Potrerillo
150 and La Colorada (Luis Torres, 2014, personal communication). Water pH ranged from 6.1
151 to 8.4 (see Table 3 in Supplemental Files).
152
153 **3. Material and methods**
154 *3.1. Coring and sampling*
155 A GARMIN GPSmap 178C Sounder was used to reconstruct the bathymetry
156 (Figure 1c) applying a Universal Kriging interpolation method (Bivand et al., 2008).
157 Seventeen short cores were retrieved along several transects in the LdM basin using a
158 hammer-modified UWITEC gravity corer during three expeditions (2011, 2012 and 2013,
159 Figure 1c, see Table 1 in Supplemental Files). Sediment cores were processed at the IPE-
160 CSIC where they were opened, imaged, described and sampled. The presence of the
161 Quizapú ash layer (1932 AD, T1, 15-17 cm depth, Figure 2a) was used as a stratigraphic
162 marker to correlate across different cores. The core LEM11-1A (0.48 m in length),
163 retrieved at the western sub-basin (43 m depth) was selected for detailed multiproxy

analyses. (Figure 1c, see Table 1 in Supplemental Files) Sedimentary facies were defined, studied and characterized based on criteria formulated by Schnurrenberger et al. (2003). After employing non-destructive logging techniques (XRF elemental analysis; see below) core LEM11-1A was sampled volumetrically in continuous 1 cm resolution intervals except for diatom samples which were taken at 3 cm resolution (1 cm thickness) and for pollen, at 4 cm resolution (1 cm thickness).

[insert Figure 2]

3.2. *Chronology*

Dating LdM sequence was challenging because the scarcity of terrestrial plant remains and the occurrence of large ^{14}C reservoir effect. Radiocarbon ages were obtained on five samples from three different cores (LEM11-1A, LEM11-3A and LEM13-3D) including macrophyte and terrestrial remains, wood and bulk sediment (see Table 1 below and Table 1 in Supplemental Files). Ages were determined by AMS ^{14}C dating at the Poznan (Poland), at the DirectAMS (USA) Accelerator Mass Spectrometry Laboratories and at UC-Irvine (Keck Radiocarbon Facility). Water at 20 m depth and living littoral aquatic macrophytes were sampled to assess the modern ^{14}C reservoir effect (Table 1).

One core, LEM12-3B (Table 1) was sampled in the field every 0.5 cm for $^{210}Pb/^{137}Cs$ (Figure 4a). The $^{137}Cs/^{210}Pb$ activities were measured by gamma-ray spectrometry, using a high-resolution low-energy coaxial HPGe detector coupled to an amplifier at St. Croix Watershed Research Station Laboratory, Science Museum of Minnesota. ^{210}Pb chronology was estimated by applying the constant rate of supply (CRS) model (Appleby, 2001). The core LEM12 -3B was correlated with adjacent LEM12-3A and with core LEM11-1A using TOC content and the T1 tephra layer horizon (Figure 4a).

3. 3. Geochemistry

An AVAATECH X-Ray Fluorescence II core scanner at the University of Barcelona was applied to core LEM11-1A at 4 mm measuring resolution using an Rh X-ray tube. Although the output includes a large number of elements (Figure 3b), Br, Al, Ti, Ca, Sr were selected to describe the changes in sediment composition. Twelve samples were analyzed using Inductively Coupled Plasma-Optical Emission Spectrometry, performed at the CEBAS-CSIC laboratory and validated by comparisons to semi quantitative XRF data (counts per second).

Elemental geochemical analyses were performed on continuous 1 cm sample intervals for total carbon (TC), total inorganic carbon (TIC) and total sulfur (TS) measured

199 in a LECO SC 144 DR furnace and for total nitrogen (TN) in a VARIO MAX CN
200 elemental analyzer. For TOC/TN_{atom} standard procedures were followed (Meyer and
201 Teranes, 2001).
202 Biosilica (BSi) analyses and measurements were performed according to Hansen
203 and Grasshoff (1983) and Mortlock and Froelich (1989) using a continuous flow
204 AutoAnalyser Technicon II. Standard procedures for precision of the biosilica
205 quantification were done (Bernárdez et al. 2005).
206
207 *3.4. Diatoms*
208 Approximately 0.15 g of dry sediment from each 13 samples, from core LEM11-
209 1A, were processed following the Queen's University methods
210 (http://post.queensu.ca/~pearl/diatoms.htm). Clastic sediments were removed using a
211 Sodium Polytungstate treatment. Microspheres were added for calculating diatom
212 concentration (Battarbee and Kneen, 1982) and permanent slides were prepared using
213 Naphrax® (Battarbee et al., 2001). Diatoms were identified and quantified under a
214 trinocular Carl Zeiss microscope, AxioLab A1 with an oil immersion objective (1000X).
215 Quantitative analyses were done by calculating relative abundances by counting
216 approximately 400 valves (up to 600 valves were counted in some levels down to 300 when

diatoms were scarce), in random fields per slide. Diatoms were classified to species or variety level (Rivera, 1970, 1974, et al., 1973; 1982; Round et al., 1990). Standard floras were used for references (Hustedt, 1961-1966; Krammer, 2000, 2002, 2003, 2009; Krammer and Lange-Bertalot, 1991, 1997; Lange-Bertalot, 1999, 2001; Levkov, 2009; Patrick and Reimer, 1966; 1975; Rumrich and Lange-Bertalot, 2000; Dunck Oliveira et al., 2012; Karthick, et al., 2012; Spaulding, et al.,1997; Van de Vijver, et al., 2010; Watanabe et al. 2012). Scanning electron microscopy (SEM LEO 1420VP in the SEM Laboratory of the Physics Department of the Pontificia Universidad Católica de Chile (http://servicios.fis.puc.cl/sem)) was employed to recognize valve ultrastructural features and diagnostic characteristics. Optical microscopy images (1000X) were taken using a digital SLR camera (Canon EOS Rebel) attached to microscope. The nomenclature status of species or variety was verified using the Catalogue of Diatom Names (California Academy of Sciences, http://researcharchive.calacademy.org/research/diatoms/names/index.asp). Diatoms were grouped according to life forms and ecological characteristics (http://westerndiatoms.colorado.edu/, and references therein: see *Aulacoseira alpigena* ecology in http://westerndiatoms.colorado.edu/taxa/species/*Aulacoseira alpigena*). Figure 5 was plotted using the Tilia software (version 2.0.19).

235

236 *3.5. Pollen*

237 Eleven pollen samples (1cm^3 sediment volume) were obtained from core LEM11-
238 1A, and processed following Faegri and Iversen (1989) methods to extract pollen grains.
239 *Lycopodium* tablets were added for calculating pollen concentration (grains/cm^3;
240 Stockmarr, 1971) and accumulation rates (grains/cm^2/ yr). Pollen grains were mounted on
241 glass slides and identified and quantified under an Axiostar Carl Zeiss microscope (400x
242 and 1000x) using published pollen atlas (Heusser, 1971; Markgraf and D'Antoni, 1978) and
243 the reference pollen collection of the Paleoecology Laboratory at CEAZA. Pollen counts
244 include 300 terrestrial pollen grains excluding paludal taxa. Relative abundances (%) are
245 presented and discussed using selected taxa which were grouped according to their
246 distribution within the vegetation belts described by Luebert and Pliscoff (2006). Pollen
247 interpretations are based on the main vegetation belts present (composition and dominant
248 species) and their elevation, according to the literature (Luebert and Pliscoff, 2006; Teillier
249 et al., 2011) (see Table 2 in Supplemental Files). Data were analyzed and plotted using
250 Tilia software (version 1.7.16)

251

252 *3.6. Data Analyses*

Analyses and charts were performed on the Open Sources software Quantum GIS and in the R Programming Language (R Core Team, 2013). Statistical treatment of data was carried out following Riani et al. (2009) and Grimm (1987).

Con formato: Inglés (Estados Unidos)

4. Results

4.1. Sedimentary facies

The LdM short cores are composed of massive to banded, brown, diatom and organic-matter -rich silts (facies D) with interspersed volcanic-rich facies (T and V) (Figure 2, 7g). In the lacustrine silts, the organic content ranges between 1-8% TOC and BSi between 9-22% (Figure 3a). Mineral fraction is mostly composed of plagioclase (60-80%), quartz (<5%), cristobalite (10-20%) minerals and glass particles (up to 20%). According to texture and composition, three main lacustrine facies have been identified. Finer facies (D1 and D2) are relatively less organic-rich (TOC: 1-2%; TS: 0.1-0.3%) and with a variable diatom content (BSi: 15-22%) (Figure 3a). D1 is finer, and with higher organic and diatom content than D2 (Figures 2, 3a). Facies D3 are banded, coarser organic-rich silts (Figures 2, 3a), with relatively higher organic matter content (TOC up to 3.5%; TS up to 0.8%) and more abundant terrestrial and littoral macrophyte remains. Layering in facies D3, defined by small changes in abundance of organic matter, coarser grain size; and the abundance of

271 macrophytes remains suggest a more littoral depositional setting for facies D3 compared to
272 D1 and D2 (Figures 2, 3a). Macrophyte-rich facies are also more common in littoral cores
273 (e.g. LEM 11-3A, 24 m water depth (Figure 2a).
274 [insert Figure 3]
275 Two main sedimentological units are defined based on facies occurrence. Basal Unit 2 (50
276 – 14 cm) is composed of facies D3, whereas the top Unit 1 (0-14 cm) is made of finer facies
277 D1 and D2. Increasing TOC values (from 1.4% to 3.5%) define subunit 2B (50-30 cm),
278 whereas relatively constant TOC values occur in 2A (30-15 cm). Low and relatively TOC
279 and TS values characterized Unit 1 (Figure 3a).
280 Up to eight volcanic-rich layers occur as cm–thick, massive, grey and dark,
281 brownish layers (Figures 2, 7g). They are composed mostly of volcanic glass, quartz and
282 plagioclase, with elevated but variable amounts of diatoms and organic remains. Based on
283 textural characteristics and composition, two main types of volcanic facies were identified:
284 T and V (Figures 2, 7g). Facies V are dark brown, with gradational boundaries and include
285 more biogenic components (organic remains, diatoms) than T, but are not present in all
286 cores. Facies V are interpreted as reworked volcanoclastic deposits, associated to increased
287 alluvial transport in the basin, of volcanic material from the watershed. Facies T (T1 and T2
288 layers) have distinctive sharp basal and upper boundaries, internal texture, dominant

289 volcanic composition and have been identified in cores throughout the lake basin. They
290 have been interpreted as ash fall deposits from recent volcanic activity. T1 is a distinctive
291 2-2.5 cm thick tephra with sharp basal and upper boundaries, and composed of a black,
292 coarser basal layer grading into finer grey layers, and it has been associated with the last
293 eruption of the Quizapú volcano in 1932 (Hildreth and Drake 1992; Ruprecht et al., 2012)
294 (Figure 2, 7g).

295 *4.2. Chronology and age model*

296 We had to use more than one analytical method (^{14}C, $^{210}Pb/^{137}Cs$, tephrochronology)
297 and several cores to obtain enough material for dating (Figure 4, Table 1). Hence, the age
298 model includes $^{137}Cs/^{210}Pb$ dating from the core LEM12-3B, two AMS ^{14}C dates from
299 wood and terrestrial plant samples from cores LEM13-3D and LEM11-1A (Table 1, Figure
300 4b). Three ^{14}C dates (on bulk organics and plant macrofossils) were obtained from core
301 LEM11-1A but only one (plant macrofossil) was used in our age model as the other two
302 clearly had a large reservoir effect. A reservoir effect is common in Andean volcanic lakes
303 and is likely caused by a large contribution of volcanic CO_2 (Geyh et al., 1999; Valero-
304 Garcés et al., 1999). We used two approaches to determine
305 [insert Figure 4]

306 this variable ^{14}C reservoir effect: i) dating the water dissolved inorganic carbon (DIC) at the
307 mixolimnion (~20 m) and modern macrophytes (Table 1), and ii) by comparing the
308 calibrated ages of ^{14}C dates to samples (^{14}C-dated or otherwise) with no reservoir effect
309 from the same stratigraphic interval (i.e. wood, the Quizapú volcano eruption of 1932 AD,
310 see Table 1, Figure 4a). Fortunately, the correlation across all of our short cores was
311 enabled by the similar TOC profiles and validated indirectly by the key presence of the
312 Quizapú eruption ash layer (Figure 2a). The DIC- based reservoir effect was similar to
313 living macrophyte (~ca. 2400 years) but considerably lower than the macrophyte-based
314 estimate based on comparison of samples from the same stratigraphic level (~ca. 4700
315 years). This variable range of the reservoir effect underlines the complexity of the carbon
316 cycle in high-altitude volcanic lakes and also suggests that biological effects on the littoral
317 realm may be significant.
318 We used a Bayesian age-depth model (Blaauw and Christen, 2011) to establish the
319 deposition rates along the core; tephra layers have been removed for the calculation since
320 they are assumed as instantaneous deposition. The final age-depth model uses Bayesian
321 statistics and includes the $^{210}Pb/^{137}Cs$ dates, Quizapu eruption (at 13 cm) and three AMS
322 dates, two without reservoir effect (wood and terrestrial plant sample from LEM13-3D (15
323 cm) and LEM11-1A (43 cm), respectively) and one with corrected values (macrophyte

macrofossil sample from LEM11-3A at 14 cm) (Figure 4b). The 1963 AD ^{137}Cs peak centered at 6.5-7 cm (Figure 4a) fits the ^{210}Pb chronology well, thus adding considerable confidence to the ^{210}Pb dating. The Pb/Cs ages estimated a sedimentation rate mean of 1.2 mm/yr for the upper Unit 1. The resulting model indicates that the core LEM11-1A spans the last 700 years (Figure 4b).

4. 3. Geochemistry

The first two components of a PCA of the XRF core scanner dataset explain ~ 80% of the variance (see Figure 5 and Table 4 in Supplemental files). The eigenvector associated with the higher eigenvalue (7.58) define two main groups of loadings: i) Rb (0.34), Zr (0.34), Zn (0.34), Ti (0.32), K (0.29), Y (0.29), Sr (0.30) and Ca (0.27) that is interpret as the volcanic input and, ii) Br (-0.30), S (-0.16), P(-0.19), Si(-0.05) and Fe (-0.04) which are related to the amount of organic matter in the sediment. The formation of iron sulfides when anoxic conditions are more dominant, explains the relationship between TOC and Fe. In addition, a significant association occurs between TOC values and Br (R2 = 0.79). As shown for other lake sequences (Gilfedder et al., 2011), Br content is associated with the amount of organic matter in the sediment, in turn a function of productivity, allocthonous input and preservation. Since most organic matter in the LdM sequence is of lacustrine origin (macrophytes and algae), in this study, the ratio Br/Ti is used as an indicator of

Con formato: Inglés (Estados Unidos)

Con formato: Inglés (Estados Unidos)

Con formato: Inglés (Estados Unidos)

organic matter content and as a reflection of bioproductivity and preservation. TOC and BSi also show good correlation (R2 = 0.48, p<0,001).

The Fe/Mn ratio is interpreted as indicator of changes in anoxic bottom conditions (Davison, 1993; Tipping et al. 1981; Wersin et al., 1991). Pronounced Mn enrichment at the top 5 cm (facies D1) and in some levels in facies D3 (35-40 cm depth) are suggestive of diagenetic Mn precipitation (Froelich et al., 1979; Kasten et al., 2003) (Figures 3b, 7f) during relatively more frequent anoxic conditions. TOC, TS and Br/Ti ratio values are higher in Unit 2 than Unit 1 reflecting an enhanced primary production and incomplete decomposition of organic matter at the lake bottom due to more frequent anoxic conditions (lower Fe/Mn ratios).

4.4. Diatoms and Biogenic Silica

233 different diatom taxa were identified from the analyze of thirteen samples, although only ten species reached a 2% in at least one level (Figure 5). Most taxa are planktonic (75.4%) and only 18.5% are benthic. The LdM diatom flora is dominated by two planktonic species *Discostella stelligera* (mean: 55.1%) and *Aulacoseira alpigena* (mean: 18.6%) as well as by a group of small fragilarioid benthic taxa (mean: 15.6%) consisting of *Staurosira construens* (dominant), *Staurosirella pinnata*, *Staurosira brevistriata*,

360 *Fragilaria pseudoconstruens*, *Pseudostaurosira brevistriata*, *Staurosira construens* var.
361 *binodis*, *Staurosirella dubia*, *Fragilaria martyi*, *Fragilaria leptostauron* var *leptostauron*,
362 and *Fragilaria* (possibly a new species). Epiphytic taxa reach a mean relative abundance of
363 0.5%. Five additional taxa exhibit relative abundances of at least 3% in at least one
364 sample, i.e., *Aulacoseira distans*, *Cyclotella meneghiniana*, *A. lirata*, epiphytic
365 *Rhoicosphenia curvata* and *Cocconeis placentula* as well as benthic *Nitzschia amphibia*
366 (Figures 3a, 5).
367 [insert Figure 5]
368 Results are summarized into groups of taxa according to their life forms (benthic,
369 epiphytic, planktonic, tychoplanktonic). The mean percentage ratio of planktonic to non-
370 planktonic (P/NP) taxa fluctuates ~ 4.7 with the lowest values at the base (61.7% of
371 planktonic taxa, ratio 1.8) and two peaks with higher values at 44-45 cm (83.3% of
372 planktonic taxa; mainly *Cyclotella* taxa, ratio: 11.8) and 16-17 cm (87.7% of planktonic
373 taxa, mainly *Cyclotella* and *Aulacoseira* taxa, P/NP ratio: 11.3, Figure 3a, 5). Total diatom
374 concentration (TDC) shows little variation (mean ~$10E^6$ valves g^{-1}) with only two peaks at
375 the base ~50 and at 17 cm (Figure 3a). BSi values show a similar pattern with higher values
376 in Unit 2 and lower values in Unit 1. Three main zones are identified based on diatom
377 assemblages.

Basal ZoneD3 (45-50 cm): the more abundant diatoms are *Discostella stelligera* (54%) and *Staurosira construens* (24.1%) (Figures 5, 3a). Planktonic diatoms show their lowest value (61.7%) (Figure 3a).

ZoneD2 (17-45 cm) shows the highest abundance of *Discostella stelligera* (59.5-78.1%), followed by *Staurosira construens* (4.9-14.8%) and *Staurosirella pinnata* (10.4%) (Figure 5). The upper part of ZoneD2 show decreasing values of *Discostella stelligera* (66.7%) and *Staurosira construens* (16%) (Figure 5).

Diatom assemblages in ZoneD1 (0-17 cm) are characterized by a co-dominance of *Discostella stelligera* (29.5-57 %), *Aulacoseira alpigena* (13.3-35.7%), and *A. distans* (32.5%) (Figure 5).

4.5. Pollen

47 pollen taxa were identified, 25 reached at least 2% in at least one level. Pollen % (Figure 6) are dominated by Poaceae throughout the record but three distinct zones are definable based on associated pollen taxa.

ZoneLEM-1 (29-48 cm depth) is dominated by Poaceae (60-51%) accompanied by mostly high Andean Low Shrubland taxa such as *Ephedra* (8.7-5.5%).

ZoneLEM-2 (18-30 cm depth) shows the highest percentages of Poaceae (61-56%) associated with increases in High Andean Steppe taxa and a decrease of pollen types associated with Low Andean Shrubland.

ZoneLEM-3 (0-18 cm) shows the most prominent change over the entire record. Poaceae % drop to 29 whereas Low Andean Shrubland and Forest taxa % increase. Exotic taxa (an indicator of human perturbations) appear and paludal taxa increase at the top.

[insert Figure 6]

5. Discussion

5.1. LdM basin processes since 1300 AD

5.1.1. Sediment delivery. Similar K, Ca and Ti profiles likely reflect the same depositional processes governing the distribution of these elements in lacustrine facies, i.e., mainly minerogenic sediment input from the surrounding watershed. Fe, Rb, Sr and Zr all follow the same overall pattern of K, Ti and Ca in Unit 1 (Figure 3b). Due to the relatively immobile characteristics of Ti, this element has been used as an indicator for clastic input (Demory et al., 2005; Haberzettl et al., 2005, 2007; Haug et al., 2003). Ca follows a similar pattern to Ti due to the presence of Ca-bearing volcanic rocks in the catchment (plagioclase), although elevated values of Al and Si (a mixed signal of allochthonous clastic

413 input and autochthonous production of biogenic silica) show a high-frequency pattern in
414 facies D1 and D2. Al values are lower in Unit 2 whereas Ti/Si fluctuates, with relatively
415 high values suggesting a higher diatom component (indicated by TDC and BSi values,
416 Figure 3a). Fluctuations in sediment delivery to the lake are associated with run-off
417 variability which in turn is related to variations in the amount and seasonality of
418 precipitation (summer vs. winter) and the duration of winter snowfall and, thus are reflected
419 in the high-frequency Ti fluctuations throughout Units 1 and 2 (Figure 3b). Periods of
420 prolonged snow cover in the catchment area reduce the annual duration of fluvial activity
421 and potentially diminish the lake clastic input. In addition, longer periods with lake water
422 stratification under snow winter accumulation and prolonged anoxic conditions at the
423 sediment/water interface, lower organic matter oxidation. This leads to higher organic
424 matter preservation and increased TOC values. Extended snow cover, however, can also
425 extend the time of snow accumulation in the catchment, leading to greater runoff during
426 snowmelt. This would result in an enhanced minerogenic flux to the lake sediments. The
427 duration of the periods of snow accumulation is likely controlled by the timing of snow
428 accumulation and melting and by winter minimum temperatures; which controls the
429 thickness of the snow layer (Livingstone, 2005). Although some minor fluctuations

occurred within Unit 2, the most significant change in LdM sequence is the relatively higher values of minerogenic input in Unit 1 compared to Unit 2.

5.1.2 Diatoms. Subfossil lake diatoms records are scarce for central Chile, the multiproxy studies from Laguna Aculeo are an exception (Jenny et al., 2002a, b) as well as a recent record from Lago Laja (Urrutia et al., 2010). Although the resolution of diatoms in LdM record is lower than geochemical proxies, it captures the centennial–scale variability and characterize the main changes within the different units.

High percentages of benthic fragilarioid taxa have been linked to cold conditions (Fey et al., 2009; Stoermer, 1993 and references therein) in many tempered lakes (Rühland et al., 2008); in LdM, a high altitude Andean lake, this relation is also seen (Figure 5, 3a). The presence of small fragilarioid (4.1-30.4%) taxa throughout the entire record, might also be indicating shallow waters in coastal areas, of circumneutral to alkaline and oligotrophic to mesotrophic (Douglas and Smol, 2010) deeper lakes (Fernández et al., 2013) (Figure 3a, 5). *Staurosira construens* and *Staurosirella pinnata* are the most abundant benthic diatoms.

Discostella. stelligera has been observed to bloom in lakes during the 20th century in relation to physical properties (ie thermal stratification (Harris et al., 2006), warmer conditions (Hyatt et al., 2011; Rühland and Smol, 2005; Rühland et al., 2003, 2010). The

448 abundance of *D. stelligera* in LdM after ~1900 AD (post LIA), decreases to almost half
449 (ZoneD1). Concordantly, LdM record shows large diatom assemblage shifts over the past
450 100 years, similar to those recorded in many lakes of the northern Hemisphere (Hyatt et al.,
451 2011; Rühland et al., 2003, 2010); although species involved are different. The shift in
452 abundance between *Discostella* and *Aulacoseira* is highly characteristic of the upper 15 cm
453 of LdM core, and is opposite to patterns described for Artic lakes during the past centuries
454 (Rühland et al., 2008). These last century changes are also prevalent in other diatom
455 records from central Chile. At Lago Laja (37.3°S) this shift is observed between *D.*
456 *stelligera*, *D.* aff. *Glomerata* and *Aulacoseira distans* which has been interpreted as a
457 combination of increases in nutrient concentrations coupled with large drops in lake level
458 during recent decades (Urrutia et al., 2010). At Laguna Aculeo (33.8°S) this shift involves
459 maximum abundance of *Melosira pseudogranulata* and *Aulacoseira granulata* and
460 minimum of *Cyclotella operculata*, which has been interpreted as increased eutrophication
461 (Cabrera and Montecino, 1982; Jenny et al., 2002a, b). Furthermore, the co-dominant
462 species in LdM record (1900 to 2011 AD) is *Aulacoseira alpigena* (3-35.7%), and although
463 it ecology is not well known, has been considered as a low-nutrient indicator. This species
464 has also been found at other high Andean lakes such as Laguna Negra and Laguna el Ocho,
465 (Alvial et al., 2008) as well as in southern Patagonia (Fernández et al., 2012). Frequent re-

suspension (enhanced mixing, Ruhland et al., 2008; Köster and Pienitz, 2006; Kilham et al., 1996) and consequently high turbidity and low light also seem to favor this species.

The late 19th century is a period of significant climate changes at a regional scale (end of the LIA, Jenny et al., 2000b) and it could have been a dominant forcing in LdM environmental change. For example, an increase in the intensity of local winds could have contributed to create turbulence in the water column, allowing *Aulacoseira* taxa (heavy silicified) to remain in the photic zone. An increased turbidity may have reduced the photic zone, leading to conditions under which better flotation and higher surface to volume exposure afforded *Aulacoseira* a greater competitive advantage (Vilaclara et al., 2010). The location of the coring site, which is relatively close to the lake margin, could also have favored more turbid conditions due to enhanced sediment delivery or re-mobilization. Although the rapid increase in *Aulacoseira* taxa occurred ~50 years prior to dam construction, early anthropogenic impacts (fishing and other early recreational uses) cannot be ruled out as an explanation for this change in diatom assemblages. In addition, damming since 1946 AD and water level management policies can affect lake hydrological properties, possibly increasing turbidity and decreasing light availability, with subsequent changes to water column mixing and stability (Rühland et al. 2010; Saros et al. 2014). The presence of *A. distans*, a typical wetland species could also be due to recent conductivity

484 changes in the lake (Camburn and Charles, 2000). In summary, the rapid changes in diatom
485 assemblages at the top of the core are likely responding to a combination of all these
486 factors.
487 At the bottom of the core at (ZoneD3) planktonic diatoms were at their lowest
488 abundance which is indicative of lower water levels.
489 Increases in epiphytic taxa (Figure 5, 3a, ZoneD1) possibly point to stronger wind
490 and wave transport of epiphytic diatoms from littoral macrophyte habitats towards the
491 coring site where they were re-deposited together with planktonic diatoms.
492 The presence of *Cyclotella meneghiniana* (ZonesD1, 2, 3) is typical of halobous to
493 oligohalobous, alkalibiont, littoral environments (Gutiérrez Téllez, 1996). The appearance
494 of *Nitzschia amphibia* (ZoneD1), although in very low abundances, could be response to
495 more eu- to hyper-eutrophic environments (Bennion, 1994; Chávez-Lara et al., 2012;
496 Hassan, 2013; Whitmore, 1989).
497 In the northern hemisphere, large 20th century changes in diatom assemblages are
498 related to climate-induced changes in the thermal regime, resulting in enhanced periods of
499 stratification and increasing productivity associated with extended growing seasons and
500 warmer conditions (Interlandi and Kilham, 2003; Rühland and Smol, 2005; Saros and
501 Anderson, 2014; et al., 2012, 2013). In the LdM record, the large change in diatom

assemblages in the upper zone is coincident with the end of the LIA (after 1850 AD) and occurs after a period of higher productivity (indicated by BSi, TDC and geochemical indicators) (Figure 3, 7e). The recent trends indicative of decreased productivity over the last decades at LdM could be associated with warming or other anthropogenic impacts and limnological perturbations. Warming temperatures and relatively higher levels after the dam construction in the 1950s would have increased the stability of the water column and might be contributing in reduced upwelling of deep-water nutrients to surface waters, thereby significantly decreasing overall lake production; although this does not explain the abundance of *Aulacoseira*. To the contrary, these taxa would decrease in abundance if the lake became more stratified after ~1900 AD. At Laguna Chica de San Pedro, Urrutia et al, (2000) provide evidence that macrophyte beds might be storing nutrients that then become unavailable for the phytoplankton. In LdM LEM11-1A record, macrophyte remains have been seen to be more abundant in facies D3 (Figure 3a), before the past century, but not in more recent facies. The recent expansion of littoral macrophyte beds, however, suggested by the increased abundance of the epiphytic diatom *Rhoicosphenia curvata* (Figure 5) could also influence biogeochemical processes, but their impact on the diatom community will need to be assessed by more research. Additionally, macrophyte-rich facies are highly abundant throughout the more littoral core LEM 11-3A (Figure 2a).

520

521 *5.1.3. Organic Bioproductivity*. The TOC/TN_{atom} fluctuates around a mean of 7 (Figure 3a)
522 and suggests a predominantly algal origin of the organic matter (between 4 - 10, Meyers
523 and Teranes, 2001). The TOC/TN_{atom} variability reflects different amounts of macrophyte
524 debris admixed with algal organic matter, (Figure 3a). As TOC, TS, TDC and BSi display a
525 rather similar pattern at LdM (Figure 3a), they are likely related to the same controlling
526 factors. These are primary productivity, dilution by minerogenic input and organic matter
527 preservation (Meyers, 2003). Silica sources are diatoms, phytoliths, chrysophytes and
528 sponge spicules and minerogenic materials. Elevated Ti/Si ratios could possibly reflect
529 higher input of Si from biosilica, an interpretation which is further supported by the TDC
530 and BSi record (Figure 3a). Hence, for the LdM record the Ti/Si ratio appears to be a
531 reliable proxy for diatom productivity as it is independent of dilution effects.
532 Changes in productivity are also controlled either by a varying influx of nutrients
533 through fluvial and/or aeolian input or the duration of open water which enables
534 photosynthesis and so controls the length of the growing season for algae and macrophytes.
535 Ti/Si, Br/Ti and BSi profiles and PC1 (Figure 3b) show coherent patterns over the
536 last 700 years interpreted as productivity (both algae and macrophyte) indicators. The
537 record presents two century-scale peaks from 1300-1400 AD and 1650-1850 AD (Figure

538 7e). Low values occur from 1400 -1650 AD as well as during most of the late 19th and 20th
539 centuries. A small increase in the last decades is marked by increases in TOC, TS, BSi,
540 Ti/Si and Br/Ti (Figures 3a, b). Endogenic carbonates are absent, although there is a level
541 with relatively high TIC (up to 1%) at between 19- 20 cm (~1800 to 1850 AD) (Figure 3b)
542 that suggests a short period of carbonate formation in the lake, possibly associated with
543 increased organic productivity.
544 [insert Figure 7]
545 *5.1.4. Vegetation changes.* The highest percentages of Poaceae and High Andean Steppe
546 taxa are suggestive of a displacement towards lower elevations of the high altitude
547 vegetation belts during zone LEM-2, compared to zone LEM-1. Although these results
548 suggest a shift towards more humid and/or cooler environmental conditions, we should be
549 cautious because of the low resolution of this sampling interval and the lack of local pollen
550 rain transects. Low pollen accumulation rates of shrubland taxa suggest decreased pollen
551 deposition, possibly associated with scarce plant cover (more typical of high altitude
552 vegetation assemblages). Moreover low pollen accumulation rates are also recorded before
553 and after LEM-2 but within the zones the values are minimal (see Figure 4 in Supplemental
554 Files). Pollen assemblages in zone LEM-3 show an increase of taxa more typical of
555 vegetation belts from lower elevations (Low Andean Shrublands and Forest taxa)

556 suggesting of a precipitation decrease and/or temperature increase. Furthermore, the
557 increase of both exotic and paludal taxa at the top of the sequence indicates anthropogenic
558 perturbation and seasonal variation of water level in the lake related to dam activities.
559 Existing records from Lago Laja (Torres et al., 2008) and Laguna de Matanzas
560 (Villa-Martínez, 2002) indicate overall drier conditions before 650 AD and from 1560 -
561 1890 AD. This contrasts with the relatively colder and moisture conditions interpreted from
562 the pollen assemblages in the LdM record (Pollen Zone LEM-2).

563 *5.2. The Little Ice Age and recent global changes in the high Andes of central Chile*

564 The LdM record provides a high resolution reconstruction of past environmental and
565 climate variations during the last 700 years in the high Andes of central Chile and can lead
566 to further assessment of the regional importance of the LIA, as well as major environmental
567 changes that occurred during the 20th century. Two periods of paleoenvironmental change
568 can be inferred across all of proxies in the LdM record. Diatom assemblages,
569 sedimentological properties and geochemical indicators (TOC, TS, Br/Ti) show a change at
570 ca ~ 1300 AD, when lower organic bioproductivity and more frequent anoxic conditions
571 occurred. The second but more significant limnological change occurred at the late 19th
572 century, when a large drop in productivity (Figure 7e) and the rapid increase of *Aulacoseira*
573 (Figure 5) mark the end of the LIA. Changes in the diatom assemblages could possible be

574 due to early anthropogenic impacts or climate factors as increased winds, that would create
575 the turbulence needed for *Aulacoseira* to remain in the photic zone and dominate the
576 phytoplankton (clearly competing with *Cyclotella* taxa, typical of thermally stratified
577 environments).
578
579 The large environmental changes seen in the LdM record are for the most part
580 coeval with other regional records in central Chile and predate the onset of colder
581 temperatures in the northern hemisphere during the LIA (Matthews and Briffa, 2005).
582 Regional records from Central Chile (De Jong et al., 2013; Von Gunten et al., 2009a;
583 Urrutia et al., 2010) show that climate was characterized by relatively colder conditions,
584 particularly cooler summers and relatively wetter conditions since 1350 AD, although
585 summer temperatures during the 18th century were significantly higher than the previous
586 interval (De Jong et al., 2013; Figure 7c). A reflectance record from Laguna Aculeo
587 indicates summer temperatures even higher than those at present from 1100 – 1350 AD
588 (Von Gunten et al., 2009a), at the end of the MCA (sensu Graham et al., 2007) and prior to
589 the onset of the LIA. This was followed by a decrease in summer temperatures of ~1°C
590 from 1350 – 1700 AD before the onset of the LIA (Von Gunten et al., 2009a). Pollen
591 records from Lago Laja and Laguna de Matanzas, as well as evidence from glacial

592 geomorphology and dendrochronology, also suggest cooler and wetter conditions between
593 1350 – 1700 AD and at ~1800 AD (Araneda et al., 2009; Espizua, 2005; Espizua y Pitte,
594 2009; Jenny et al., 2002a; Le Quesne et al., 2009; Neukom et al., 2010, 2011; Urrutia et al.,
595 2010; Villa-Martínez, 2004; Von Gunten et al., 2009b). Further evidence for a cold episode
596 during the LIA comes from a record of glacial advance between 1550 – 1720 AD from the
597 same region as the LdM (Espizua 2005; Espizua y Pitte 2009). The LIA thus stands out as a
598 time of significant and complex hydrological, environmental and climate change in central
599 Chile.

600 In contrast, dendrochronological records taken along the western Andean slope
601 between 32-38 °S show that the last 100 yrs are also some of the driest of the last few
602 centuries (Christie et al., 2010; Le Quesne et al., 2006, 2009). Geochemical proxies at LdM
603 indicate that a large decrease in productivity occurred towards the end of the 19th century,
604 although dominant anoxic conditions appeared to have remained at the lake bottom. Pollen
605 assemblages (Low Andean Shrublands and Forest taxa) suggest a precipitation decrease
606 and/or temperature increase in the 20th century. An increase also in exotic and paludal taxa
607 may indicate seasonal variations of the water level in the lake related to dam management.
608

609 Over the last decades, the LdM record evidences a dominance of *Aulacoseira* in the
610 diatom communities, a possible increase in the development of littoral macrophyte
611 meadows and a slight recovery of bioproductivity (relatively higher TOC, Br/Ti, BSi,
612 Ti/Si). The increase in the trophic state of the lake could be related to an increase in actual
613 nutrient loading as a consequence of sport fishing and outdoor human activities. The
614 development of macrophyte meadows suggested by the recent appearance of the epiphytic
615 diatom *Rhoicosphenia curvata* (Figure 5) is coherent with an increase in the extent of
616 shallow lake environments as shown in other lake systems (Balls et al., 1989). This could
617 be related to the extensive flooding of shallow areas after the dam construction in the 1950s
618 and the water management regime for irrigation and hydropower generation. Lower values
619 of TDC for recent decades (Figure 3a), however, suggest that the planktonic (mainly
620 *Cyclotella* and *Aulacoseira* taxa) productivity has decreased although littoral productivity
621 (macrophytes) may have increased (Figure 7e). Macrophytes could act sequestering
622 nutrients, with consequent lowering of phytoplankton productivity, but this hypothesis
623 requires further confirmation; pointing to a complex pattern of productivity changes in
624 LdM.
625 Another factor to consider is the higher temperatures recorded for the recent decades
626 of global warming in the high Andes of continental Chile (Falvey and Garreaud, 2009). In

central and northern Chile (17°–37°S) *in situ* temperature observations confirm the strong contrast between cooling off the coast (0.2 °C/decade) and warming in the central valley and western Andes (+0.25°C/decade), only 100 – 200 km further inland (and 500 – 2500 m higher in elevation). The warming rate along the western slope of the Andes is similar to that observed on the eastern (continental) slopes.

Warmer temperatures in the high Andes are related to a shorter duration of the snowpack of the LdM in recent decades, and are conducive to an early melting of the snow cover, increased runoff and meltwater discharge into the lake during spring and early summer, and more turbulent conditions in coastal areas. This, between other factors, could be evidenced by the presence of *Aulacoseira* taxa, although it could also be indicating windier conditions and/or higher water levels (Fernández et al., 2012).

What drives the centennial scale environmental changes visible in the Laguna del Maule record? Although many features of the LdM record are in accordance with global variations in climate (i.e. colder climates at the onset of LIA, recent 20th century warming) others appear to be clearly regional and not global in extent (onset of colder, anoxic conditions and decreased productivity during the early 15th century, and increased temperatures, oxic conditions and productivity during the 18th century). In Patagonia,

changes in the location and intensity of the Westerlies have been considered as the main forcing for dry/wet phases during the LIA (Moy et al., 2008; Moreno et al., 2014) associated to reduced Hadley circulation during period of reduced solar activity (Chambers et al., 2014). In LdM region, moisture changes during the last centuries should be related to winter precipitation variability, mostly controlled by the intensity and location of the South Pacific High and changes in ENSO dynamics (Garreaud, 2009). The possible link with solar irradiance and ENSO dynamics of the internal LIA variability shown in LdM record needs to be explore with high resolution records from the Andes and other areas where human impact was minimal until the mid-20th century.

6. Conclusions

The history of Laguna del Maule over the past 700 years has been reconstructed based on sedimentological, geochemical and biological indicators. Geochemical proxies (Fe/Mn, S/Ti) show more frequent oxic bottom conditions prior to 1400 AD followed by a general trend to increased anoxic conditions, punctuated by a phase of higher oxygenation between 1650 – 1850 AD. In LdM record, periods of increased productivity indicated by Br/Ti and Ti/Si (1300 – 1400 AD and 1650 – 1850 AD) correspond with phases of decreased anoxia, likely associated to lower lake levels and occurred during periods of

663 climate transition to and from colder states that signified prominent changes in summer
664 temperature throughout central Chile and southern South America. Past variations in lake
665 limnology and hydrology coincide in part with the Little Ice Age (with cooler/wetter
666 conditions from 1570 to 1700 AD and a final phase ending ca. 1850 AD) but also indicate
667 major environmental change in the 18th century, seen in other records across central Chile
668 and northern Patagonia. Both, anthropogenic and climate factors are likely responsible for
669 recent changes in LdM basin. Introduction of new species due mainly to fishing activities,
670 increased turbulence of the water column and changes in the thermal stratification caused
671 by the damming and warmer conditions, could all contribute to the changes seen in diatom
672 assemblages in the 20th century. These recent changes have no previous analog in the past
673 700 years and indicate a possible environmental shift in the lake towards an unprecedented
674 state.
675
676 **Acknowledgements**
677 We thank A.L. Herrera for help with diatom samples, H. Orellana, F. Barreiro
678 Lostres, F.P. Díaz and L. Torres (the "Alcalde de Mar" at Laguna del Maule) for their help
679 and logistical support in the field; M. Soto-Herrera (SEM Lab.), N. Serrano (Dirección de
680 Obras Hidráulicas) and P. Zavala (curator, PUC) for technical help.
681

Funding

This work was supported by FONDECYT (Chile) [Grant No. 3120012], the Ministry of Economy and Competitiveness (Spain) [Grant No. CGL2012-32501] to HOLOCHILL and the Institute of Ecology and Biodiversity (Chile) through [grants ICM P05-002 and PFB-23].

References

Ahmed KF, Wang G, Silander J, Wilson AM, Allen JM, Horton R, Anyah R (2013) Statistical downscaling and bias correction of climate model outputs for climate change impact assessment in the U.S. northeast. *Global Planetary Change* 100: 320-332.

Ahn J, Brook EJ, Schmittner A, Kreutz K (2012) Abrupt change in atmospheric CO2 during the last ice age. *Geophysical Research Letters* 39: L18711. Doi:10.1029/2012GL053018, 2012.

Alvial I, Cruces FJ, Araneda AE, Grosjean M, Urrutia RE (2008) Diatoms community structure in superficial sediments of eight Andean lakes of central Chile. *Revista Chilena de Historia Natural* 81: 83-94.

Appleby PG (2001) Chronostratigraphic techniques in recent sediments. In: Last, W.L., Smol, J.P. (Eds.), Tracking Environmental Change Using Lake Sediments. Basin

700 Analysis, Coring, and Chronological Techniques. *Developments in*
701 *Paleoenvironmental Research*. Kluwer Academic Publishers, Dordrecht: 171–203.
702 Appleby PG, Oldfield F (1978) The calculation of ^{210}Pb dates assuming a
703 constant rate of supply of unsupported ^{210}Pb to the sediment. *Catena* 5:1-8.
704 Araneda A, Torrejón F, Aguayo M, Alvial I, Mendoza C, Urrutia R (2009) Historical
705 records of Cipreses glacier (34ºS): combining documentary-inferred "Little Ice Age"
706 evidence from Southern and Central Chile. *The Holocene* 19(8):1173-1183.
707 Arias Reyes CS (2011) *Análisis de los efectos de distintos escenarios de registro histórico*
708 *en la estimación de caudales de crecida. aplicación a obras hidráulicas de la*
709 *cuenca del río Maule*. Memoria de Título, Universidad de Chile, Chile.
710 Balls HR, Moss B, Irvine K (1989) The loss of submerged plants on eutrophication. I.
711 Experimental design, water chemistry, aquatic plant and phytoplankton biomass in
712 experiments carried out in ponds in the Norfolk Broadland. *Freshwater Biology* 22:
713 71–87.
714 Battarbee RW, Kneen MJ (1982) The use of electronically counted microspheres in
715 absolute diatom analysis. *Limnology and Oceanography* 27(l): 184-188.
716 Battarbee RW, Jones VJ, Flower RJ, Cameron NG, Bennion H, Carvalho L, Juggins S
717 (2001) Diatoms. In: Last WM, Smol JP, (eds.), *Tracking environmental change*

718 *using lake sediments, 3: Terrestrial, algal and siliceous indicators*, Kluwer
719 Academic Publishers, Dordrecht: 155–202.
720 Bennion H (1994) A diatom-phosphorus transfer function for shallow, eutrophic ponds in
721 south-east England. *Hydrobiologia* 275(6): 391-410.
722 Bernárdez P, Prego R, Francés G, González-Álvarez R (2005) Opal content in the Rła de
723 Vigo and Galician continental shelf: biogenic silica in the muddy fraction as an
724 accurate paleoproductivity proxy. *Continental Shelf Research* 25: 1249–1264.
725 Bivand RS, Pebesma EJ, Gómez-Rubio V (2008) Applied spatial data analysis with R.
726 (Vol. 747248717). Springer.
727 Blaauw M, Christen JA (2011) Flexible paleoclimate age-depth models using an
728 autoregressive gamma process. *Bayesian Analysis* 6: 457-474.
729 Boes X, Fagel N (2008) Relationships between southern Chilean varved lake
730 sediments, precipitation and ENSO for the last 600 years. *Journal of*
731 *Paleolimnology* 39: 237–252. DOI 10.1007/s10933-007-9119-9.
732 Cabrera S, Montecino V (1982) Eutrophy of lake Aculeo. *Plant and Soil* 67: 377–387.
733 Camburn KE, Charles DF (2000) *Diatoms of low-alkalinity lakes in the northeastern*
734 *United States*. Academy of Natural Sciences.

Con formato: Inglés (Estados Unidos)

Con formato: Inglés (Estados Unidos)

735 Chambers, FM, Brain SA, Mauquoy D, McCarroll J, Daley T (2014) The 'Little Ice Age'
736 in the Southern Hemisphere in the Context of the Last 3000 Years: Peat-Based
737 Proxy-Climate Data from Tierra Del Fuego. *The Holocene* 24(12): 1649–56.
738 doi:10.1177/0959683614551232.
739 Chávez-Lara CM, Priyadarsi DR, Caballero MM, Carreño AL, Chokkalingam L (2012)
740 Lacustrine ostracodes from the Chihuahuan Desert of Mexico and inferred Late
741 Quaternary paleoecological conditions. *Revista Mexicana de Ciencias Geológicas*
742 29(2): 422-431.
743 Christie DA, Boninsegna JA, Cleaveland MK, Lara A, Le Quesne C, Morales MS,
744 Mudelsee M, Stahle DW, Villalba R (2010) Aridity changes in the Temperate-
745 Mediterranean transition of the Andes since 1346 AD reconstructed from tree-rings.
746 *Climate Dynamics* 36(7-8):1505-1521. Doi:10.1007/s00382-009-0723-4.
747 Crowley TJ, Zielinski G, Vinther B, Udisti R, Kreutz K, Cole-Dai J., Castellano E (2008)
748 Volcanism and the Little IceAge, PAGES Newsletter 16: 22–23.
749 Crutzen PJ, Stoermer EF (2000) The "anthropocene". IGBP's Global Change Newsletter
750 41: 17–18.
751 Davison W (1993) Iron and manganese in lakes. *Earth-Science Reviews* 34(2): 119–163.

Con formato: Inglés (Estados Unidos)

752 Dirección de Obras Hidráulicas (DOH), Ministerio de Obras Públicas (MOP). Available
753 online at: www.doh.gob.cl/Paginas/default.aspx.
754 De Jong R, Von Gunten L, Maldonado A, Grosjean M (2013) Late Holocene summer
755 temperatures in the central Andes reconstructed from the sediments of high-
756 elevation Laguna Chepical, Chile (32° S). *Climate of the Past* 9: 1921–1932.
757 Delaygue G, Bard E (2010) An Antarctic view of beryllium-10 and solar activity for the
758 past millennium. *Climate Dynamics* 36: 2201–2218.
759 Demory F, Nowaczyk NR, Witt A, Oberhansli H (2005) High-resolution magneto-
760 stratigraphy of late Quaternary sediments from Lake Baikal, Siberia: timing of
761 intracontinental paleoclimatic responses. *Global and Planetary Change* 46: 167–
762 186.
763 Douglas MSV, Smol JP (2010) Freshwater diatoms as indicators of environmental change
764 in the High Artic. In: Smol JP, Stoermer EF (eds) The diatoms: applications for the
765 environmental and earth sciences, 2nd edn. Cambridge University Press,
766 Cambridge: 249–266.
767 Dunck Oliveira B, de Souza Nogueira I, Machado Souza MG (2012) *Stenopterobia* e
768 *Surirella* (Bacillariophyceae, Surirellaceae) do Sistema Lago dos Tigres, Britânia,
769 Goiás. *Rodriguésia* 63(3): 525-539.

770 Espizua LE (2005) Holocene glacier chronology of Valenzuela Valley, Mendoza Andes,
771 Argentina. *The Holocene* 15(7): 1079-1085.
772 Espizua LE, Pitte P (2009) The Little Ice Age glacier advance in the Central Andes (35°S),
773 Argentina. *Palaeogeography, Palaeoclimatology, Palaeoecology* 281:345–350.
774 Faegri K, Iversen J (1989) *Textbook of pollen analysis.* 4ª ed. × K Faegri, PE Kaland and K
775 Krzywinski. John Wiley and Sons.
776 Fagel N, Bertrand S, Mattielli N, Gilson D, Chirinos L, Lepoint G, Urrutia R (2010)
777 Geochemical evidence (C, N and Pb isotopes) of recent anthropogenic impact in
778 south-central Chile from two environmentally distinct lake sediment records.
779 *Journal of Quaternary Science* 25 : 1100–1112.
780 Falvey M, Garreaud R (2009) Regional cooling in a warming world: Recent temperature
781 trends in the SE Pacific and along the west coast of subtropical South America
782 (1979-2006). *Journal of Geophysical Research* 114(D04102): 1-16.
783 Doi:10.1029/2008JD010519.
784 Feigl KL, Le Mevel H, Ali ST, Córdova L, Andersen NL, DeMets C, Singer BS (2014)
785 Rapid uplift in Laguna del Maule volcanic field of the Andean Southern Volcanic
786 Zone (Chile) 2007–2012. *Geophysical Journal International* 196(2):885–901.
787 doi:10.1093/gji/ggt438.

788 Fernández M, Maidana N, Rabassa J (2012) Palaeoenvironmental conditions during the
789 Middle Holocene at Isla de los Estados (Staaten Island, Tierra del Fuego, 54 S,
790 Argentina) and their influence on the possibilities for human exploration.
791 *Quaternary International* 256: 78-87.
792 Fernández M, Bjorck S, Wohlfarth B, Maidana N, Unkel I, Van der Putten N (2013)
793 Diatom assemblage changes in lacustrine sediments from Isla de los Estados,
794 southernmost South America, in response to shifts in the southwesterly wind belt
795 during the last deglaciation. *Journal of Paleolimnology* 50: 433–446.
796 Fey M, Korr C, Maidana N, Carrevedo M, Corbella H, Dietrich S, Haberzettl T, Kuhn G,
797 Lücke A, Mayr C, Ohlendorf C, Paez M, Quintana F, Schäbitz F, Zolitschka B
798 (2009) Palaeoenvironmental changes during the last 1600 years inferred from the
799 sediment record of a cirque lake in southern Patagonia Laguna Las Vizcachas,
800 Argentina. *Palaeogeography, Palaeoclimatology, Palaeoecology* 281(3): 363-375.
801 Fournier TJ, Pritchard ME, Riddick SN (2010) Duration, magnitude, and frequency of
802 subaerial volcano deformation events: new results from Latin America using InSAR
803 and a global synthesis. *Geochemistry, Geophysics, Geosystems* 11: 1-29.
804 Dx.doi.org/10.1029/2009GC002558.

805 Fourtanier E, Kociolek, JP (on-line version updated: 19 September of 2011). Catalogue of
806 Diatom Names, California Academy of Sciences. Available online at
807 http://research.calacademy.org/research/diatoms/names/index.asp.
808 Fritz SC (2008) Deciphering climatic history from lake sediments. *Journal of*
809 *Paleolimnology* 39: 5-16.
810 Froelich PN, Klinkhammer GP, Bender ML, Luedtke NA, Heath GR, Cullen D, Dauphin P,
811 Hammond D, Hartman B, Maynard V (1979) Early oxidation of organic matter in
812 pelagic sediments of the eastern Atlantic: suboxic diagenesis. *Geochimica et*
813 *Cosmochimica Acta* 43: 1075-1090.
814 García Berguecio N (2006) *Comparative floristic analysis of the high-Andean vegetation of*
815 *the coastal and Andes mountain ranges of central Chile*. Memoria de Título,
816 Universidad de Chile, Chile.
817 Garreaud R (2009) The Andes climate and weather. Advances in Geosciences 7: 1-9.
818 Geyh M, Grosjean M, Nuñez LA, Schotterer U (1999) Radiocarbon reservoir effect and the
819 timing of the Late-Glacial/Early Holocene humid phase in the Atacama Desert,
820 Northern Chile. *Quaternary Research* 52: 143–153.

821 Gilfedder BS, Petri M, Wessels M, Biester H (2011) Bromine species fluxes from Lake
822 Constance's catchment, and a preliminary lake mass balance. *Geochimica et*
823 *Cosmochimica Acta* 75: 3385–3401.
824 Graham NE, Hughes MK, Ammann CM, Cobb KM, Hoerling MP, Kennett DJ, Kennett JP,
825 Rein B, Stott L, Wigand PE, Xu T (2007) Tropical Pacific mid-latitude
826 teleconnections in medieval times. *Climate Change* 83:241–285.
827 Grimm EC (1987) CONISS: A Fortran 77 program for stratigraphically constrained cluster
828 analysis by the method of incremental sum of squares. *Computers & Geosciences*
829 13(1): 13-35.
830 Gutiérrez Téllez BM (1996) Diatomeas del Pleistoceno de Pehuen-Có (Provincia de
831 Buenos Aires): Inferencias Paleoambientales. *Ameghiniana* 33(2): 201-208.
832 Haberzettl T, Fey M, Lucke A, Maidana N, Mayr C, Ohlendorf C, Schabitz F,
833 Schleser GH, Wille M, Zolitschka B (2005) Climatically induced lake level
834 changes during the last two millennia as reflected in sediments of Laguna
835 Potrok Aike, southern Patagonia (Santa Cruz, Argentina). *Journal of*
836 *Paleolimnology* 33: 283–302.
837 Haberzettl T, Corbella H, Fey M, Janssen S, Lucke A, Mayr C, Ohlendorf C,

Con formato: Inglés (Estados Unidos)

Con formato: Inglés (Estados Unidos)

838 Schabitz F, Schleser GH, Wille M, Wulf S, Zolitschka B (2007a) Late glacial and
839 Holocene wet-dry cycles in southern Patagonia: chronology, sedimentology and
840 geochemistry of a lacustrine record from Laguna Potrok Aike, Argentina. *The*
841 *Holocene* 17: 297–310.
842 Haberzettl T, Mayr C, Wille M, Zolitschka B (2007b) Linkages between Southern
843 Hemisphere Westerlies and hydrological changes in semi-arid Patagonia during the
844 last 16,000 years. *PAGES News* 15: 22–23.
845 Hansen HP, Grasshoff K (1983) Procedures for the automated determination of seawater
846 constituents. In: Grasshoff K, Ehrhardt M and Kremling K (eds) *Methods of*
847 *seawater analysis* (second, revised and extended edition). Verlag Chemie,
848 Weinheim, pp. 362-379.
849 Harris MA, Cumming BF, Smol JP (2006) Assessment of recent environmental changes in
850 New Brunswick (Canada) lakes based on paleolimnological shifts in diatom species
851 assemblages. *Canadian Journal of Botany-Revue Canadienne de Botanique* 84(1):
852 151-163.
853 Hassan, GS (2013) Diatom-based reconstruction of Middle to Late Holocene
854 paleoenvironments in Lake Lonkoy, southern Pampas, Argentina. *Diatom Research*
855 28(4): 473–486, dx.doi.org/10.1080/0269249X.2013.851118.

Con formato: Inglés (Estados Unidos)

856 Haug, GH, Gunther D, Peterson LC, Sigman DM, Hughen KA, Aeschlimann B (2003)
857 Climate and the collapse of Maya civilization. *Science* 299: 1731-1735.
858 Heusser C, 1971. *Pollen and Spores of Chile*. The University of Arizona Press, Tucson.
859 Hildreth W, Drake RE (1992) Volcán Quizapú, Chilean Andes. *Bulletin of Volcanology* 54:
860 93-125.
861 Hildreth W, Godoy E, Fierstein J, Singer B (2010) *Laguna del Maule Volcanic Field:*
862 *Eruptive History of a Quaternary Basalt to Rhyolite Distributed Volcanic Field on*
863 *the Range crest in Central Chile.* Boletin Servicio Nacional de Geología y Minería
864 Chile 63, Santiago, Chile.
865 Hustedt F (1961-1966) Die Kieselalgen. In: Rabenhorst L (ed), *Kryptogamen-flora von*
866 *Deutschland, Osterreich und der Schweiz*, 7(2) 6: 737 -845 (1959); 7(3) 1: 1 - 160
867 (1961); 7(3) 2: 161 – 348 (1962); 7(3) 4: 557 - 816.
868 Hyatt CV, Paterson AM, Rühland KM, Smol JP (2011) Examining 20th century water
869 quality and ecological changes in the Lake of the Woods, Ontario, Canada: A
870 paleolimnological investigation. *Journal of Great Lakes Research* 37: 456–469.
871 Interlandi SJ, Kilham, SS (2003) Diatom-chemistry relationships in Yellowstone Lake
872 (Wyoming) sediments: Implications for climatic and aquatic processes research.
873 *Limnology and Oceanography* 18(1): 79-92.

874 IPCC (Intergovernmental Panel on Climate Change) Fourth Assessment Report: Climate
875 Change (AR4) (2007) Contribution of Working Groups I, II and III to the Fourth
876 Assessment Report of the Intergovernmental Panel on Climate Change Core.
877 Writing Team, Pachauri RK and Reisinger A (Eds), IPCC, Geneva, Switzerland.
878 IPCC Contribution of Working Group I to the Fourth Assessment Report (2007) Solomon
879 S, D Qin, M Manning, Z Chen, M Marquis, KB Averyt, M Tignor and HL Miller
880 (eds) Cambridge University Press, Cambridge, United Kingdom and New York,
881 NY, USA.
882 IPCC Working Group III Contribution to AR5. Climate Change (2014) Mitigation of
883 Climate Change.
884 Jenny B, Valero-Garcés BL, Villa-Martínez R, Urrutia R, Geyh M, Veit H (2002a). Early to
885 Mid-Holocene Aridity in Central Chile and the Southern Westerlies: The Laguna
886 Aculeo Record (34°S). *Quaternary Research* 58(2): 160-170.
887 Jenny B, Valero-Garces BL, Urrutia R, Kelts K, Veit H, Appleby PG, Geyh M (2002b)
888 Moisture changes and fluctuations of the Westerlies in Mediterranean Central Chile
889 during the last 2000 years: The Laguna Aculeo record (33 degrees 50 ' S).
890 *Quaternary International* 87: 3-18.

Jenny B, Wilhelm D, Valero-Garces BL (2003) The Southern Westerlies in Central Chile: Holocene precipitation estimates based on a water balance model for Laguna Aculeo (33degrees 50 ' S). *Climate Dynamics* 20: 269-280.

Karthick B, Hamilton PB, Kociolek PJ (2012) Taxonomy and biogeography of some *Surirella* Turpin (Bacillariophyceae) taxa from Peninsular India. *Nova Hedwigia* 141: 81–116.

Kasten S, Zabel M, Heuer V, Hensen C (2003) Processes and signals of non-steady state diagenesis in deep-sea sediments and their pore waters. In: *The South Atlantic in the Late Quaternary: Reconstruction of material budget and current systems,* Wefer G, Mulitza S and Ratmeyer V (eds), Springer, pp. 431-459.

Kilham SS, Theriot EC, Fritz SC (1996) Linking planktonic diatoms and climate change in the large lakes of Yellowstone ecosystem using resource theory. *Limnology and Oceanography* 41:1052–1062.

Köster D, Pienitz R (2006) Late-Holocene environmental history of two New England ponds: natural dynamics versus human impacts. *The Holocene* 16: 519-532.

Krammer K (2000) The genus *Pinnularia*. In: *Diatoms of Europe. Diatoms of the European Inland Waters and Comparable habitats*. Lange Bertalot H (ed), Vol 1. Koenigstein. ARG Gantner Verlag K.G.

909 Krammer K (2002) *Cymbella*. In: Diatoms of Europe. Diatoms of the European Inland
910 Waters and Comparable habitats. H. Lange Bertalot (ed.). Vol 3. Koenigstein. ARG
911 Gantner Verlag K.G.
912 Krammer K (2003) *Cymbopleura*, *Delicata*, *Navicymbula*, *Gomphocymbellopsis*,
913 *Afrocymbella*. In: Diatoms of Europe. Diatoms of the European Inland Waters and
914 Comparable Habitats. H. Lange-Bertalot (ed.). Vol. 4: Koenigstein. A. R. G.
915 Gantner Verlag K.G.
916 Kramer K (2009) *Diatoms of Europe, Vol 3, Cymbella*. Edited by H. Lange- Bertalot,
917 Gantner, Ruggell.
918 Krammer K, Lange-Bertalot H (1991) *Süßwasserflora von Mitteleuropa,*
919 *Bacillariophyceae, 4.Teil: Achnanthaceae, Kritische Ergänzungen zu Achnanthes*
920 *s.l, Navicula s. str., Gomphonema.* Elsevier, Berlin.
921 Krammer K, Lange-Bertalot H (1991) *Süßwasserflora von Mitteleuropa,*
922 *Bacillariophyceae, 3.Teil: Centrales, Fragilariaceae, Eunotiaceae*. Elsevier, Jena.
923 Krammer K, Lange-Bertalot H (1997) *Süßwasserflora von Mitteleuropa,*
924 *Bacillariophyceae, 1.Teil: Naviculaceae*. Elsevier, Jena.

925 Krammer K, Lange-Bertalot H (1997) *Süβwasserflora von Mitteleuropa,*
926 *Bacillariophyceae, 2.Teil: Bacillariaceae, Ephitemiaceae, Surirellaceae*. Elsevier,
927 Berlin.
928 Lange-Bertalot H (1999) Neue Kombinationen von Taxa aus *Achnanthes* Bory (sensu lato).
929 *Iconographia Diatomologica* 6: 278-291.
930 Lange-Bertalot H (2001) *Diatoms of Europe. Navicula sensu stricto. 10 Genera Separated*
931 *from Navicula sensu lato. Frustulia*. Ed. Lange-Bertalot, H., Ruggell.
932 Latorre C, Moreno PI, Vargas G, Maldonado A, Villa-Martínez R, Armesto JJ, Villagrán C,
933 Pino M, Núñez L, Grosjean M (2007) Late Quaternary environments and
934 palaeoclimate. *The Geology of Chile*, Gibbons W, Moreno T (Eds), The London
935 Geological Society Press, London, Great Britain: 311-330.
936 Le Quesne C, Stahle DW, Cleaveland MK, Therrell MD, Aravena JC, Barichivich J (2006)
937 Ancient Austrocedrus tree-ring chronologies used to reconstruct Central Chile
938 precipitation variability from A.D. 1200 to 2000. *Journal of Climate* 19: 5731–
939 5744.
940 Le Quesne C , Acuña C, Boninsegna JA, Rivera A, Barichivich J (2009) Long-term glacier
941 variations in the Central Andes of Argentina and Chile, inferred from historical

records and treering reconstructed precipitation. *Palaeogeography, Palaeoclimatology, Palaeoecology* 281: 334–344.

Levkov Z (2009) *Diatoms of Europe, Vol 5, Amphora* sensu lato. Edited by H. Lange-Bertalot, Gantner, Liechtenstein.

Livingstone DM (2005) Ice cover on lakes and rivers. Climate trends inferred from historical records. *EAWAG News* 58: 19–22.

Luebert F, Pliscoff P (2006) *Sinopsis bioclimática y vegetacional de Chile.* Editorial Universitaria, Santiago.

Matthews JA, Briffa KR (2005) The "Little Ice Age," reevaluation of an evolving concept. Geografiska Annaler. Series A, *Physical Geography* 87: 17-36.

Markgraf V, D'Antoni HL (1978) Pollen flora of Argentina. University of Arizona Press.

Meyers PA (2003) Applications of organic geochemistry of paleolimnological reconstructions: a summary of examples from the Laurentian Great Lakes. *Organic Geochemistry* 34: 261−289.

Meyers PA, Teranes, JL (2001) Sediment organic matter. In: Last WM, Meyers PA, Teranes JL (eds) *Tracking environmental change using lake sediments*, vol. 2: Physical and geochemical methods. Kluwer, pp. 239–265.

Con formato: Inglés (Estados Unidos)

959 Montecinos A, Kurgansky MV, Muñoz C, Takahashi K (2011) Non-ENSO interannual
960 rainfall variability in central Chile during austral winter. *Theoretical & Applied*
961 *Climatology* 106 (3-4): 557, DOI:10.1007/s00704-011-0457-1.
962 Moreno PI, Vilanova I, Villa-Martínez R, Garreaud RD, Rojas M, De Pol-Holz R (2014)
963 Southern Annular Mode-like changes in southwestern Patagonia at centennial
964 timescales over the last three millennia. *Nature communications*, 5.
965 Mortlock RA, Froelich PN (1989) A simple method for the rapid determination
966 of biogenic opal in pelagic marine sediments. *Deep Sea Research Part A.*
967 *Oceanographic Research Papers* 36:1415–1426.
968 Moy CM, Dunbar RB, Moreno PI, Francois JP, Villa-Martínez R, Mucciarone DM,
969 Guilderson TP, Garreaud RD (2008) Isotopic evidence for hydrologic change
970 related to the westerlies in SW Patagonia, Chile, during the last millennium.
971 *Quaternary Science Reviews*, 27(13): 1335-1349.
972 Neukom R, Luterbacher J, Villalba R, Küttel M, Frank D, Jones PD, Grosjean M, Esper J,
973 Lopez L, Wanner H (2010) Multi-centennial summer and winter precipitation
974 variability in southern South America. *Geophysical Research Letters* 37: L14708.
975 Neukom R, Luterbacher J, Villalba R, Kuttel M, Frank D, Jones PD, Grosjean M, Wanner
976 H, Aravena JC, Black DE, Christie DA, D'Arrigo R, Lara A, Morales M, Soliz-

Con formato: Inglés (Estados Unidos)

Con formato: Inglés (Estados Unidos)

977 Gamboa, C, Srur A, Urrutia R, Von Gunten L (2011) Multiproxy summer and
978 winter surface air temperature field reconstructions for southern South America
979 covering the past centuries. *Climate Dynamics* 37(1–2):35–51. Doi:10.1007/s00382-
980 010-0793-3.
981 Patrick R, Reimer CW (1966) *The diatoms of the United States.Vol. 1: Fragilariaceae,*
982 *Eunotiaceae, Achnanthaceae, Naviculaceae*. Academy of Natural Sciences of
983 Philadelphia Monography.
984 Patrick R, Reimer CW (1975) *The diatoms of the United States (exclusive of Alaska and*
985 *Hawaii)*. Academy of Natural Sciences of Philadelphia Monography, 13(2), 1-213.
986 Quintana JM, Aceituno P (2012) Changes in the rainfall regime along the extratropical west
987 coast of South America (Chile): 30-43º S. *Atmosfera* 25(1): 1-22.
988 R Development Core Team (2013) R: A language and environment for statistical
989 computing. R Foundation for Statistical Computing, Vienna, Austria. ISBN 3-
990 900051-07-0. Available at: www.R-project.org.
991 Riani M, Atkinson AC, Cerioli A (2009) Finding an unknown number of multivariate
992 outliers. *Journal of the Royal Statistical Society* 71(2): 447–466.
993 Rivera P (1970) Diatomeas de los lagos Ranco, Laja y Laguna Chica de San Pedro (Chile).
994 *Gayana Botánica* 20: 1-23.

995 Rivera P (1974) Diatomeas de agua dulce de Concepción y alrededores (Chile). *Gayana*
996 *Botánica* 28: 1-134.
997 Rivera P, Parra O, González M (1973) Fitoplancton del estero Lenga (Chile). *Gayana*
998 *Botánica* 23: 1-93.
999 Rivera P, Parra O, González M, Dellarossa V, Orellana M (1982) *Manual Taxonómico del*
1000 *fitoplancton de aguas continentales*. Editorial Universidad de Concepción,
1001 Concepción.
1002 Rodhe H, Grennfelt P, Wisniewski J, Agren C, Bengtsson G, Johansson K, Kauppi P,
1003 Kucera V, Rasmussen L, Rosseland B, Schotte L, Sellden G (1995) Acid reign '95?
1004 —conference summary statement. *Water Air and Soil Pollution* 85: 1–14.
1005 Round FE, Crawford RM, Mann DE (1990) *The Diatoms. Biology and Morphology of the*
1006 *Genera*. Cambridge University Press, Cambridge.
1007 Rühland K, Karst T, Paterson A, Gregory-Eaves R, Smol JP, Cumming BF (1999)
1008 *Standard Sediment Sample Preparation Methods for Siliceous Microfossils*
1009 *(Diatoms and Chrysophyte Scales and Cysts).* PEARL Paleoecological
1010 Environmental Assessment and Research Laboratory Department of Biology,
1011 Queen's University, Kingston ON, Canada, K7L 3N6. Available at:
1012 post.queensu.ca/~pearl/diatoms.htm.

1013 Rühland K, Priesnitz A, Smol JP (2003) Paleolimnological Evidence from Diatoms for
1014 Recent Environmental Changes in 50 Lakes across Canadian Arctic Treeline.
1015 *Arctic, Antarctic, and Alpine Research* 35(1): 110–123.
1016 Rühland, K., Smol, J.P. (2005) Diatom shifts as evidence for recent Subarctic warming in a
1017 remote tundra lake, NWT, Canada. *Palaeogeography, Palaeoclimatology,*
1018 *Palaeoecology* 226: 1– 16.
1019 Rühland K, Paterson AM, Smol JP (2008) Hemispheric-scale patterns of climate-related
1020 shifts in planktonic diatoms from North American and European lakes. *Global*
1021 *Change Biology* 14: 2740–2754.
1022 Rühland K, Paterson AM, Hargan K, Jenkin A, Clark BJ, Smol JP (2010) Reorganization of
1023 algal communities in the Lake of the Woods (Ontario, Canada) in response to turn-
1024 of-the-century damming and recent warming. *Limnology and Oceanography* 55(6):
1025 2433–2451.
1026 Rumrich U, Lange-Bertalot H (2000) *Iconographia Diatomologica, Diatomeen der Anden*,
1027 A.R.G Gantner Verlag K.G, Rugell.
1028 Ruprecht P, Bergantz G, Cooper K, Hildreth W (2012) The crustal magma storage system
1029 of Volcan Quizapú, Chile, and the effects of magma mixing on magma diversity.
1030 *Journal of Petrology*. Doi:10.1093/petrology/egs002.

1031 Sandoval Jeria J (2003) *El riego en Chile*. Gobierno de Chile Ministerio de Obras Públicas,
1032 Dirección de Obras Hidráulicas.
1033 Saros JE, Anderson NJ (2014) The ecology of the planktonic diatom *Cyclotella*
1034 and its implications for global environmental change studies. *Biological Reviews*.
1035 Doi: 10.1111/brv.12120.
1036 Saros JE, Stone JR, Pederson GT, Slemmons KEH, Spanbauer T, Schliep A, Cahl D,
1037 Williamson CE, Engstrom DR (2012) Climate-induced changes in lake ecosystem
1038 structure inferred from coupled neo- and paleoecological approaches.
1039 *Ecology* 93(10): 2155–2164.
1040 Saros JE, Strock KE, McCue1 J, Hogan E, Anderson NJ (2013) Response of *Cyclotella*
1041 species to nutrients and incubation depth in Arctic lakes. *Journal of Plankton*
1042 *Research* 36(2): 450-460. Doi:10.1093/plankt/fbt126.
1043 Schnurrenberger D, Russell J, Kelts K (2003) Classification of lacustrine sediments based
1044 on sedimentary components. *Journal of Paleolimnology* 29: 141-154.
1045 Smol JP (2008) *Pollution of lakes and rivers. A paleoenvironmental perspective*. Blackwell
1046 Publishing Ltd, Malden.

1047 Spaulding SA, McKnight DM, Stoermer EF, Doran PT (1997) Diatoms in sediments of
1048 perennially ice-covered Lake Hoare, and implications for interpreting lake history in
1049 the McMurdo Dry Valleys of Antarctica. *Journal of Paleolimnology* 17: 403–420.
1050 Spaulding SA, Lubinski DJ, Potapova M (2010) *Diatoms of the United States*. Available at:
1051 westerndiatoms.colorado.edu.
1052 Stockmarr J (1971) Tablets with spores used in absolute pollen analysis. *Pollen spores* 13:
1053 615-621.
1054 Stoermer EF (1993) Evaluating diatom succession: some peculiarities of the Great Lakes
1055 case. *Journal of Paleolimnology* 8: 71–83.
1056 Teillier S, Marticorena A, Niemeyer, H (2011) *Flora Andina de Santiago. Guía para la*
1057 *identificación de las especies de las cuencas del Maipo y del Mapocho.* Universidad
1058 de Chile.
1059 Tipping E, Woof C, Cooke D (1981) Iron oxide from a seasonally anoxic lake. *Geochimica*
1060 *et Cosmochimica Acta* 45(9): 1411–1419.
1061 Torres L, Parra O, Araneda A, Urrutia R, Cruces F, Chirinos L (2008) Vegetational and
1062 climatic history during the late Holocene in Lake Laja basin (central Chile) inferred
1063 from sedimentary pollen record. *Review of Palaeobotany and Palynology* 149:18-
1064 28.

1065 Trenberth, KE, Fasullo JT (2013) An apparent hiatus in global warming? *Earth's Future* 1:
1066 19–32.
1067 Urrutia R, Cisternas M, Araneda A, Retamal O, Parra O, Mardones M (2000)
1068 Caracterización morfométrica y sedimentológica de cinco lagos costeros de la VIII
1069 Región, Chile. *Revista Geográfica de Chile Terra Australis*. 45: 7-24.
1070 Urrutia R, Sabbe K, Cruces F, Pozo K, Becerra J, Araneda A, Vyverman W, Parra O (2000)
1071 Paleolimnological studies of Laguna Chica of San Pedro (VIII Region): diatoms,
1072 hydrocarbons and fatty acid records. Revista Chilena de Historia Natural 73: 717–
1073 728.
1074 Urrutia R, Araneda A, Torres L, Cruces F, Vivero, C, Torrejón F, Barra R, Fagel N, Scharf
1075 B (2010) Late Holocene environmental changes inferred from diatom, chironomid,
1076 and pollen assemblages in an Andean lake in Central Chile, Lake Laja (36 S).
1077 *Hydrobiologia* 648: 207–225. DOI 10.1007/s10750-010-0264-1.
1078 Valero-Garcés BL, Grosjean M, Kelts K, Schreier H, Messerli B (1999) Holocene
1079 Lacustrine Deposition in the Atacama Altiplano: Facies Models, Climate and
1080 Tectonic Forcing. *Palaeogeography, Palaeoclimatology, Palaeoecology* 151(1):
1081 101–125.

1082 Van de Vijver B, Mataloni G, Stanish L, Spaulding SA (2010) New and interesting species
1083 of the genus *Muelleria* (Bacillariophyta) from the Antarctic region and South
1084 Africa. *Phycologia* 49(1): 22–41.
1085 Viale M, Garreaud R (2014) Summer precipitation events over the western slope of the
1086 subtropical Andes. *Monthly Weather Review* 142: 1074-1092. DOI: 10.1175/MWR-
1087 D-13-00259.1.
1088 Vilaclara G, Martinez-Mekler G, Cuna E, Ugalde E (2010.) Diatom-inferred
1089 palaeoenvironmental changes of a Pliocene lake disturbed by volcanic activity.
1090 *Journal of Paleolimnology* 44: 203-215.
1091 Villa-Martínez R (2002) *Historia del clima y la vegetación de Chile Central durante el*
1092 *Holoceno: una reconstrucción basada en el análisis de polen, sedimentos,*
1093 *microalgas y carbón*. Unpublished PhD Thesis, Universidad de Chile, Chile.
1094 Villa-Martínez R, Villagrán C, Jenny B (2004). Palynological evidence for Late Holocene
1095 climate variability from Laguna de Aculeo, Central Chile (lat.34°S). *The Holocene*
1096 14:361-367.
1097 Von Gunten L, Grosjean M, Rein B, Urrutia R, Appleby P (2009a) A quantitative high-
1098 resolution summer temperature reconstruction based on sedimentary pigments from
1099 Laguna Aculeo, central Chile, back to AD 850. *The Holocene* 19(6): 873–881.

Von Gunten L, Grosjean M, Eggenberger U, Grob P, Urrutia R, Morales A (2009b) Pollution and eutrophication history AD 1800–2005 as recorded in sediments from five lakes in Central Chile. *Global and Planetary Change* 68: 198–208.

Von Gunten L, Grosjean M, Beer J, Grob, P., Morales, A., Urrutia R (2009c) Age modeling of young non-varved lake sediments: methods and limits. Examples from two lakes in Central Chile. *Journal of Paleolimnology.* DOI 10.1007/s10933-008-9284-5.

Watanabe T, Mayama S, Idei M (2012) Overlooked heteropolarity in *Surirella* cf. *fastuosa* (Bacillariophyta) and relationships between valve morphogenesis and auxospore development. *Journal of Phycology* : 1–13.

Wersin P, Hohener P, Giovanoli R, Stumm W (1991) Early diagenetic influences on iron transformations in a freshwater lake sediment. *Chemical Geology* 90: 233-252.

Whitmore T (1989) Florida diatoms assemblages as indicators of trophic state and pH. *Limnology and Oceanography* 34: 882-895.

Figure captions

Figure 1. (a) Location of Laguna del Maule (LdM) in central Chile and other sites mentioned in the text. (b) Maule River hydrographic watershed and location of Quizapu

volcano. (c) LdM bathymetric map showing core location (2011, 2012 field campaigns) dam location and watershed topography.

Figure 2. (a) Short sediment core transect in LdM: LEM11-2A, LEM11-1A, LEM11-3A, LEM 12-3A, LEM12-3B, LEM12-4A. Sedimentary facies, TOC, radiocarbon dates and correlation using elemental composition profiles and T1 tephra. The inset shows the bathymetric map shows the location of cores used in this manuscript and the dam location. (b) Lithological description of core LEM11-1A.

Figure 3. (a) Sedimentological, compositional geochemical, diatom data, facies and stratigraphic units for core LEM11-1A. (b) Core LEM11-1A XRF data (counts per second). PC1 and a CONISS analysis (plotted to the right) (see text for explanation). Dam construction (1946-1958 AD) is also indicated.

TS: total sulfur

TOC: total organic carbon

TIC: total inorganic carbon

TOC/TN_{atom}: total organic carbon/total nitrogen ratio

BSi: Biosilica

TDC: total diatom concentration

Plank/non plank: planktonic/non-planktonic ratio

P: % of planktonic diatoms

B: % of benthic diatoms

Sf: % of small fragilarioid

XRF: X-ray fluorescence

PC1: score plot of the first component (70% of total variance) for PCA analysis of XRF data

Figure 4. LdM age model with dates from cores LEM11-1A, LEM12-3A and LEM12-3B. (a) Correlation between sediment cores LEM12-3A and LEM12-3B using TOC profiles and the Quizapú ash fall tephra. Right inset: ^{137}Cs-^{210}Pb dating using the CRS model (Appleby and Oldfield, 1978) (core LEM12-3B, ^{137}Cs peak at 7 cm). Stars indicate the location of radiocarbon dates. (b) A Bayesian age-depth model (Blaauw and Christen, 2011) based on three AMS ^{14}C from cores LEM11-1A (terrestrial plants), LEM11-3A (aquatic macrophytes, with a calculated reservoir effect of 4700 yrs) and LEM13-3D (wood sample), ^{137}Cs-^{210}Pb dating from core LEM12-3B and the Quizapú ash layer (1932). See text for details.

Figure 5. Diatom record from LdM. Relative abundances (> 1%) of diatom species present in core LEM11-1A. CONISS analysis facies and stratigraphic units.

PLNK: planktonic taxa

TYCH: tychoplanktonic taxa

BNTH: benthic taxa

EPPH: epiphytic taxa

Figure 6. Pollen record from LdM. Relative abundances (%) of major pollen taxa present in core LEM11-1A.CONISS analysis, facies and stratigraphic units.

Figure 7. A comparison of the LdM record with global, regional and local records: (a) reconstruction of Total Solar Irradiance (TSI) (after Delaygue and Bard, 2010) and volcanic aerosols (AOD) based on Antarctic sulphate records (Crowley et al., 2008); (b) reconstruction of South America temperature anomalies from the PAGES 2K initiative (after Ahmed et al., 2013); (c) a temperature reconstruction from the Andes of central Chile (L. Chepical 32ºS, 3000 m, after De Jong et al., 2013); (d) a temperature reconstruction from the central valley of Chile (L. Aculeo, 34ºS, 350 m, after Von Gunten et al., 2009);

(e) the Laguna del Maule record including proxies for productivity (Br/Ti and Ti/Si); (f) redox conditions (Fe/Mn) and organic versus clastic influence (PC1, from XRF data related to the organic matter and volcanic input in the sediment (see Supplementary Files Fig 5 and Table 4); (g) thickness of volcanic facies of LdM.

LIA: Little Ice Age (after Matthews and Briffa, 2005)

PAGES: Past Global Changes

DAM: time since dam construction.

Con formato: Inglés (Estados Unidos)

Table 1. AMS radiocarbon dates from Laguna del Maule.

Lab. Code	CORE	Depth (cm)	Sample type	^{14}C yr BP	Error (δ)	Cal yr BC/AD (Median)	Error BC/AD (lower)	Error BC/AD (upper)
Poz-59915	LEM11-3A	14	Macrophyte macrofossil	4820	60	-3559	-3662	-3374
Poz-57545	LEM13-3D	15	Wood	85	25	1891	1704	1945
UCIAMS 133686	LEM11-1A	30	Bulk sediment	4760	15	-3506	-3632	-3376
UCIAMS 133687	LEM11-1A	43	Terrestrial plant macros	680	35	1351	1291	1395
D-AMS 001135	LEM11-1A	47	Bulk sediment	4367	25	-2937	-3021	-2889
Poz-57281	LEM 13-20m	*	DIC water	2370	30	-397	-515	-257
Poz-60705	LEM 135D	*	Modern macrophytes	2380	30	-403	-537	-265

1184

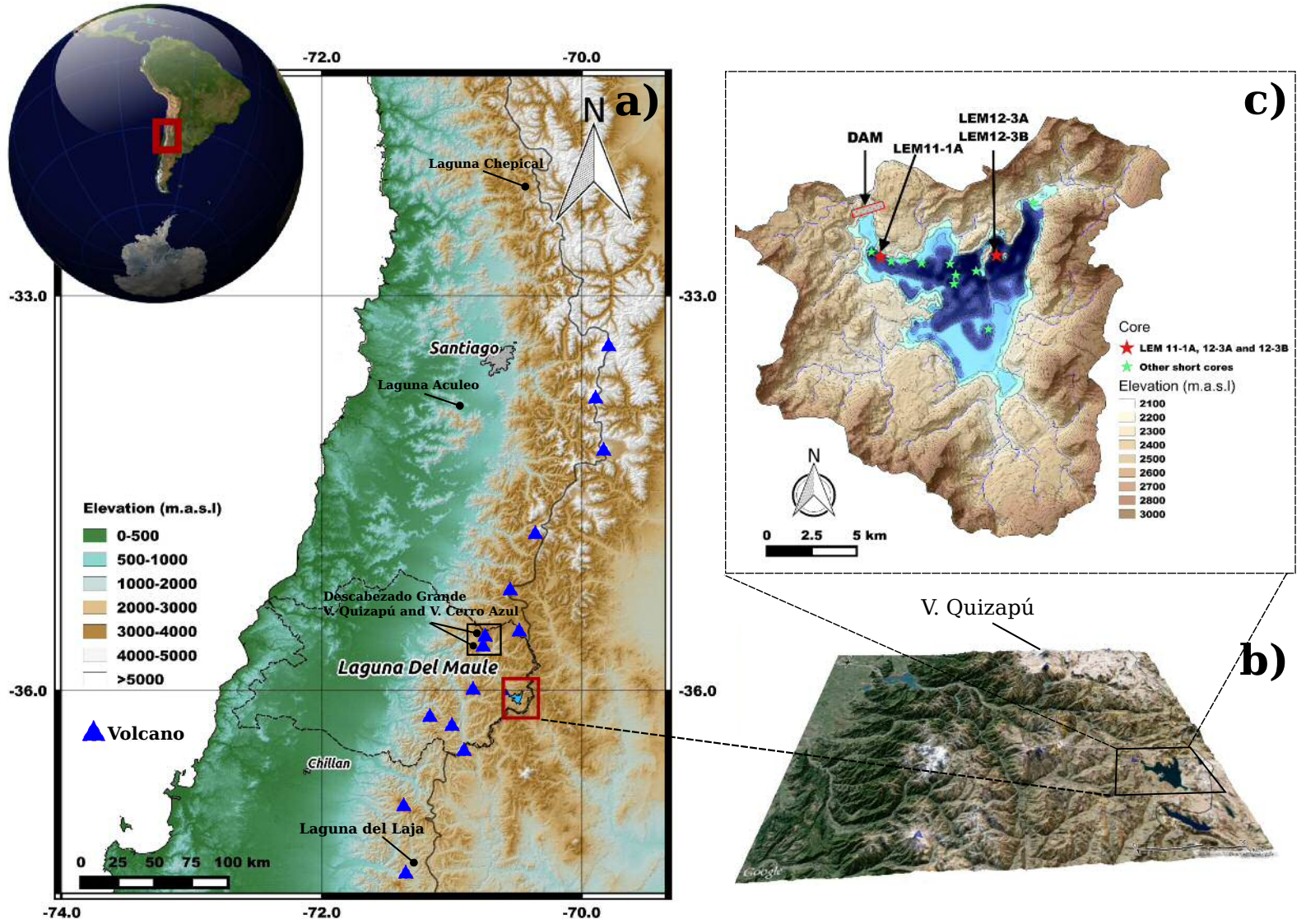
a)
-72.0
-70.0
-33.0
-36.0
-74.0
N
Laguna Chepical
Santiago
Laguna Aculeo
Descabezado Grande
V. Quizapú and V. Cerro Azul
Laguna Del Maule
Chillan
Laguna del Laja
Volcano
Elevation (m.a.s.l)
0-500
500-1000
1000-2000
2000-3000
3000-4000
4000-5000
>5000
0 25 50 75 100 km
c)
DAM
LEM11-1A
LEM12-3A
LEM12-3B
Core
LEM 11-1A, 12-3A and 12-3B
Other short cores
Elevation (m.a.s.l)
2100
2200
2300
2400
2500
2600
2700
2800
3000
0 2.5 5 km
V. Quizapú
b)
Google

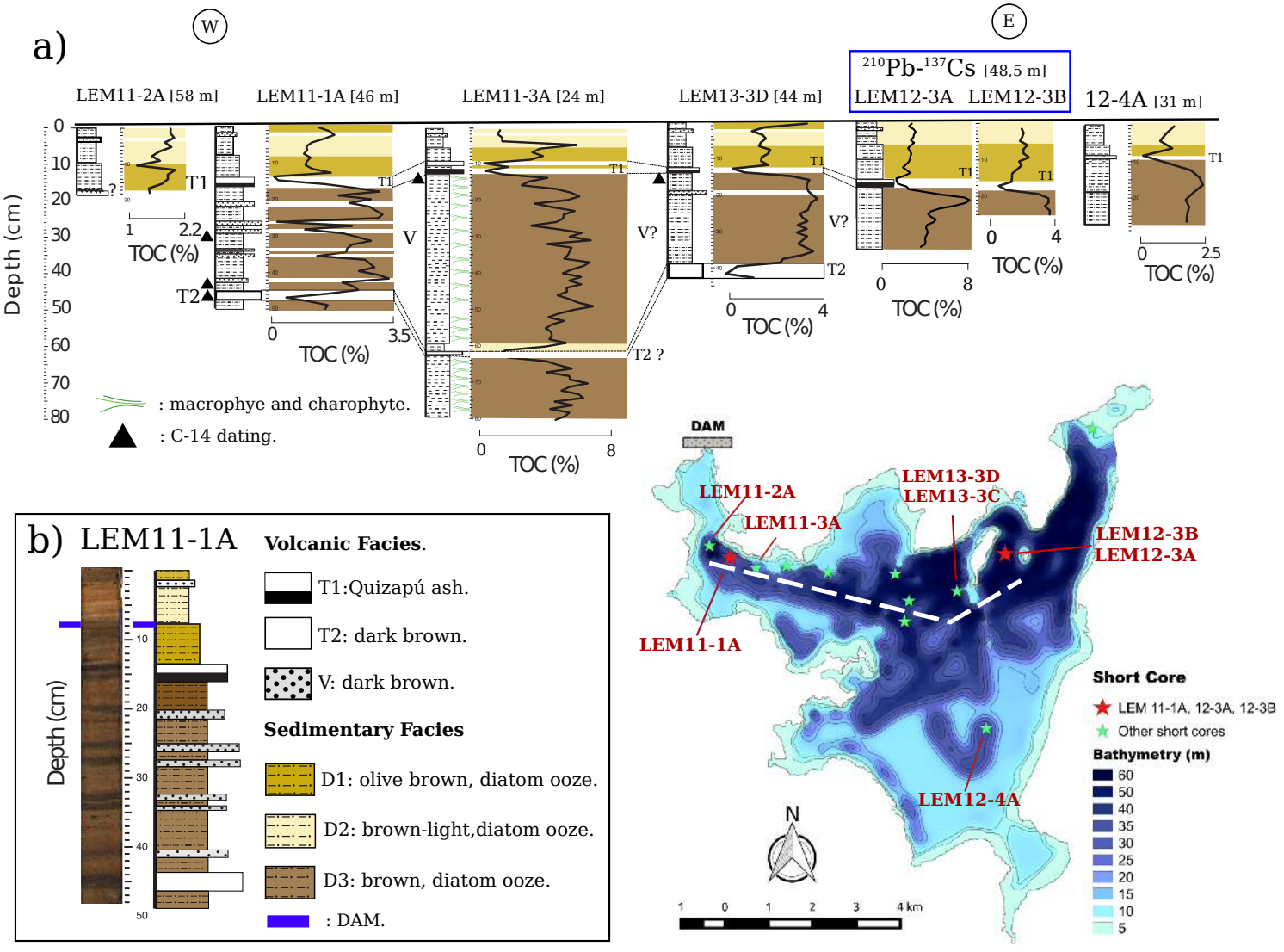
a)
W
E
LEM11-2A [58 m]
LEM11-1A [46 m]
LEM11-3A [24 m]
LEM13-3D [44 m]
210Pb-137Cs [48,5 m]
LEM12-3A LEM12-3B
12-4A [31 m]
Depth (cm)
T1
T2
V
V?
T2 ?
TOC (%)
: macrophye and charophyte.
: C-14 dating.
b) LEM11-1A
Volcanic Facies.
T1:Quizapú ash.
T2: dark brown.
V: dark brown.
Sedimentary Facies
D1: olive brown, diatom ooze.
D2: brown-light,diatom ooze.
D3: brown, diatom ooze.
: DAM.
DAM
LEM11-2A
LEM11-3A
LEM13-3D
LEM13-3C
LEM12-3B
LEM12-3A
LEM11-1A
LEM12-4A
N
4 km
Short Core
LEM 11-1A, 12-3A, 12-3B
Other short cores
Bathymetry (m)
60
50
40
35
30
25
20
15
10
5

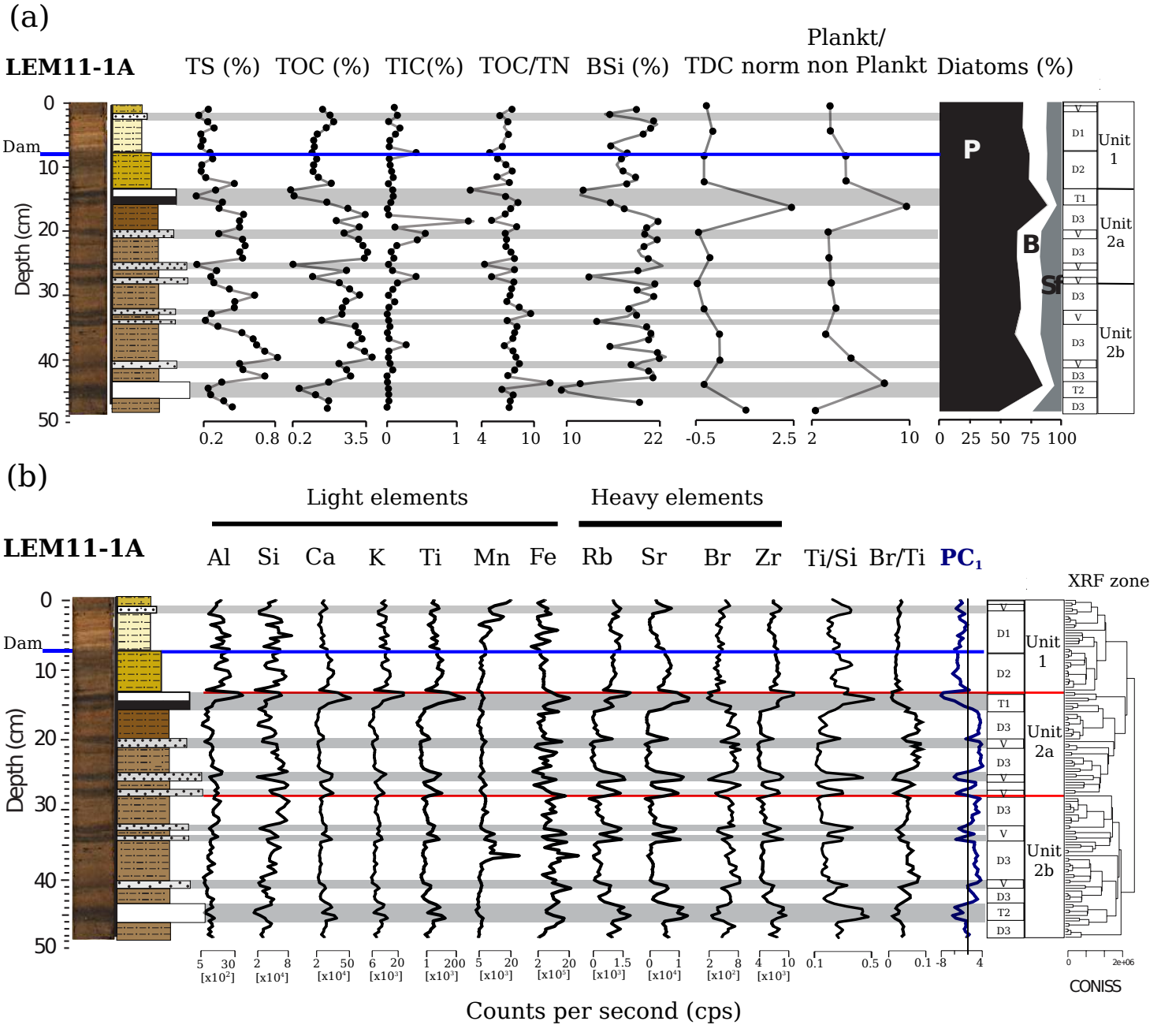
(a)
LEM11-1A
TS (%)
TOC (%)
TIC(%)
TOC/TN
BSi (%)
TDC norm
Plankt/ non Plankt
Diatoms (%)
Dam
Depth (cm)
P
B
Unit 1
Unit 2a
Unit 2b
(b)
Light elements
Heavy elements
LEM11-1A
Al
Si
Ca
K
Ti
Mn
Fe
Rb
Sr
Br
Zr
Ti/Si
Br/Ti
PC1
XRF zone
CONISS
Counts per second (cps)

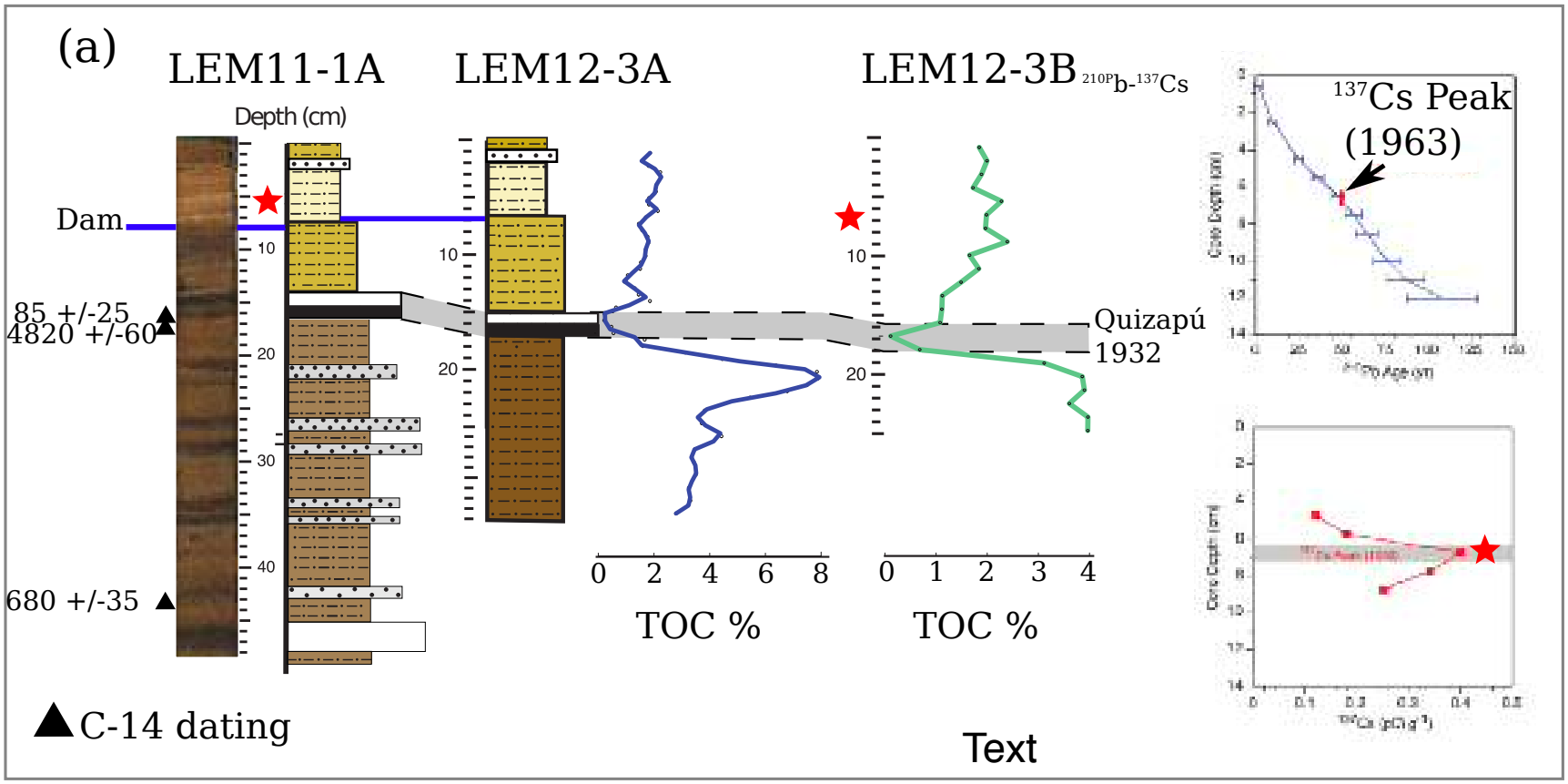
(a)
LEM11-1A
LEM12-3A
LEM12-3B
210Pb-137Cs
Depth (cm)
Dam
85 +/-25
4820 +/-60
680 +/-35
C-14 dating
TOC %
TOC %
Quizapú
1932
137Cs Peak
(1963)

Text

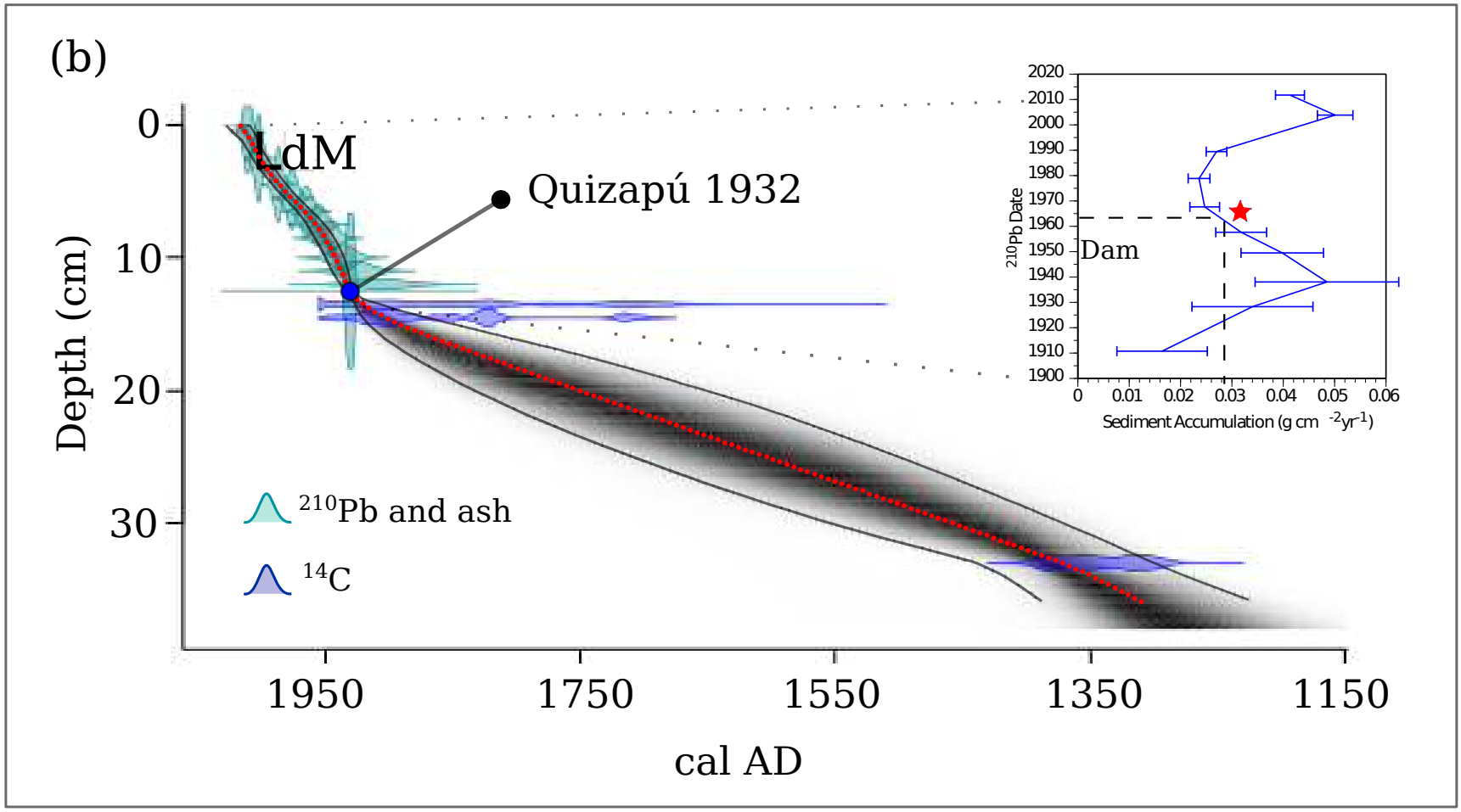
(b)
LdM
Quizapú 1932
Depth (cm)
210Pb and ash
14C
cal AD
210Pb Date
Dam
Sediment Accumulation (g cm -2yr-1)

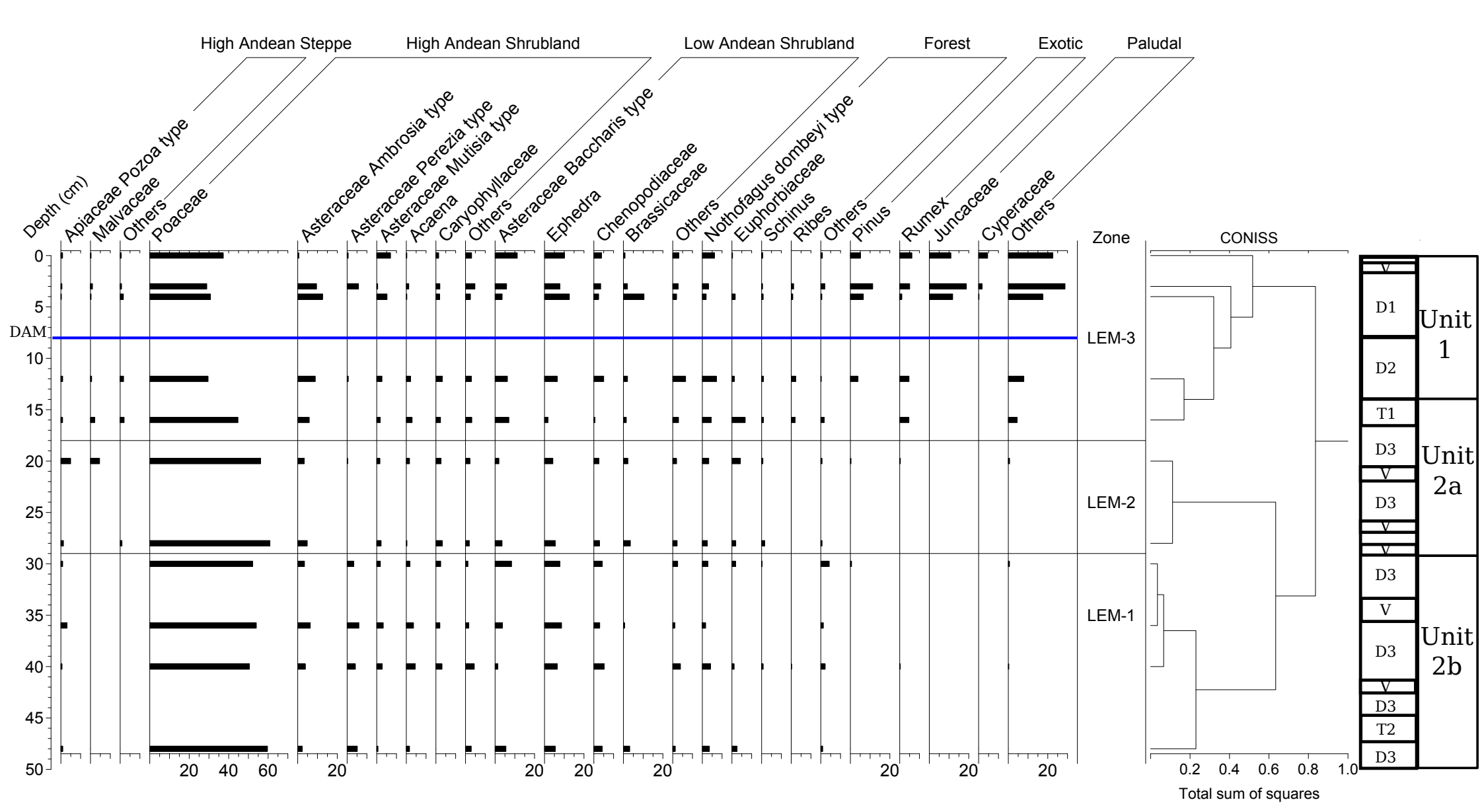
High Andean Steppe
High Andean Shrubland
Low Andean Shrubland
Forest
Exotic
Paludal
Depth (cm)
Apiaceae Pozoa type
Malvaceae
Others
Poaceae
Asteraceae Ambrosia type
Asteraceae Perezia type
Asteraceae Mutisia type
Acaena
Caryophyllaceae
Others
Asteraceae Baccharis type
Ephedra
Chenopodiaceae
Brassicaceae
Others
Nothofagus dombeyi type
Euphorbiaceae
Schinus
Ribes
Others
Pinus
Rumex
Juncaceae
Cyperaceae
Others
Zone
CONISS
DAM
LEM-3
LEM-2
LEM-1
0
5
10
15
20
25
30
35
40
45
50
20
40
60
0.2
0.4
0.6
0.8
1.0
Total sum of squares
V
D1
D2
T1
D3
V
D3
V
V
D3
V
D3
V
D3
T2
D3
Unit 1
Unit 2a
Unit 2b

Diatoms of Laguna del Maule (LEM11-1A)

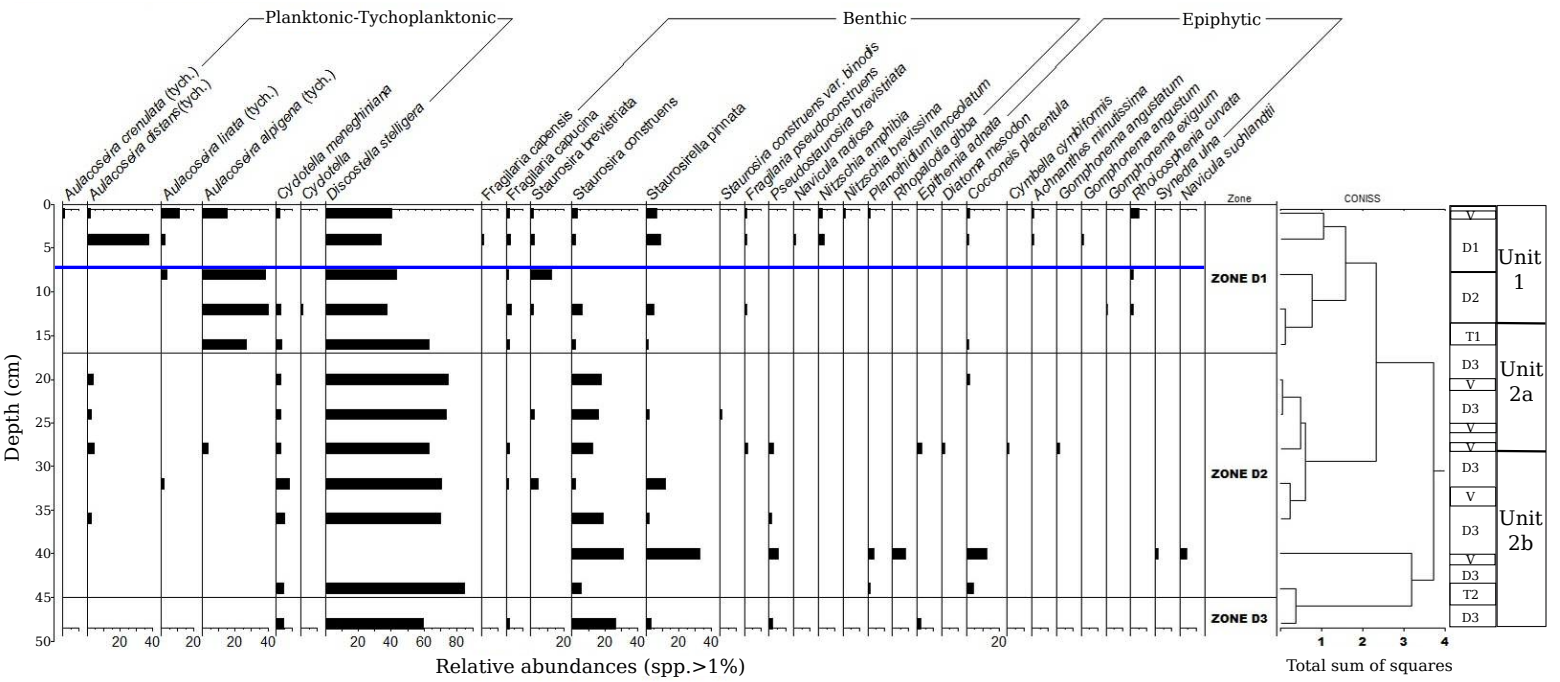

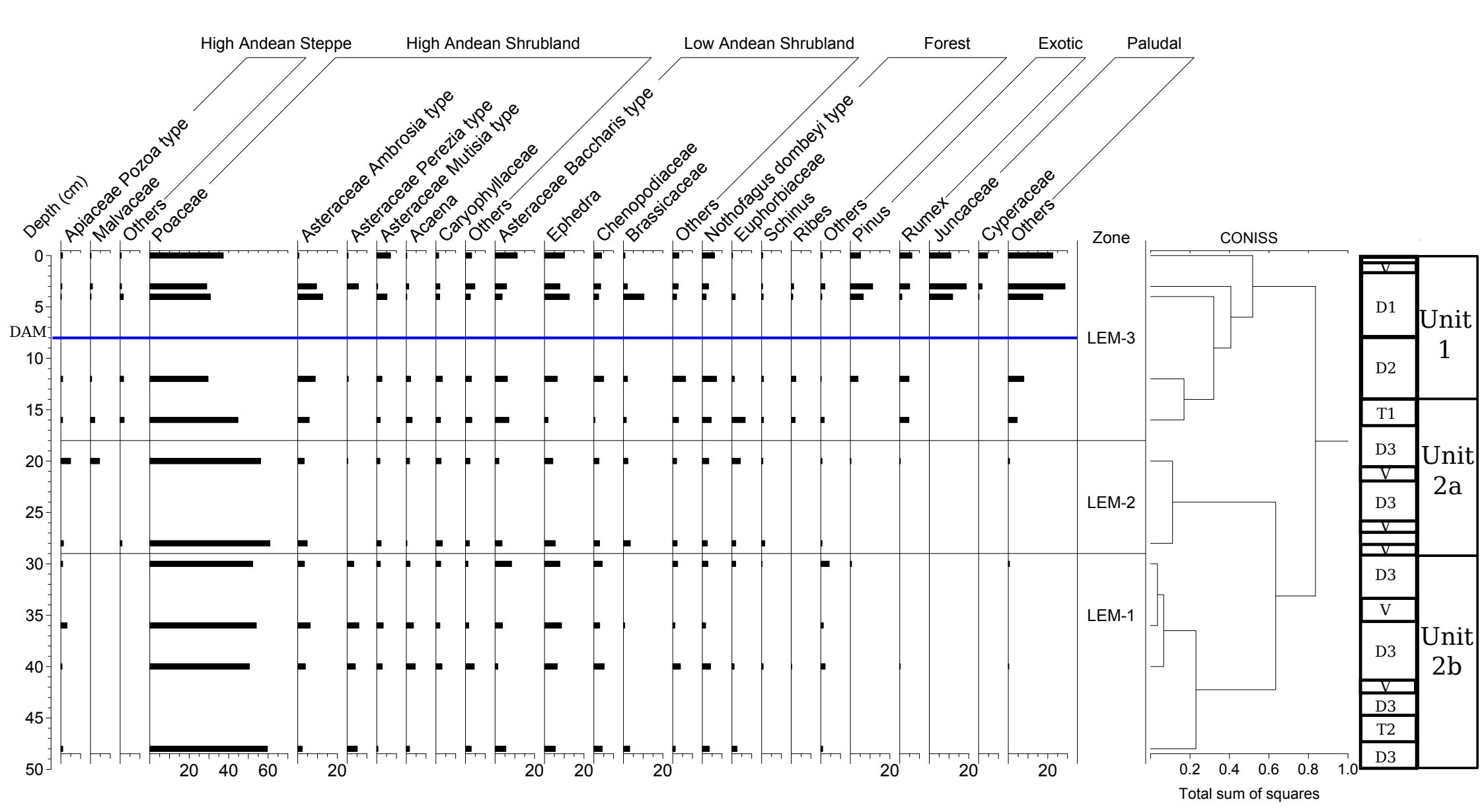
High Andean Steppe
High Andean Shrubland
Low Andean Shrubland
Forest
Exotic
Paludal
Depth (cm)
Apiaceae Pozoa type
Malvaceae
Others
Poaceae
Asteraceae Ambrosia type
Asteraceae Perezia type
Asteraceae Mutisia type
Acaena
Caryophyllaceae
Others
Asteraceae Baccharis type
Ephedra
Chenopodiaceae
Brassicaceae
Others
Nothofagus dombeyi type
Euphorbiaceae
Schinus
Ribes
Others
Pinus
Rumex
Juncaceae
Cyperaceae
Others
Zone
CONISS
DAM
LEM-3
LEM-2
LEM-1
0
5
10
15
20
25
30
35
40
45
50
20
40
60
0.2
0.4
0.6
0.8
1.0
Total sum of squares
V
D1
D2
T1
D3
V
D3
V
V
D3
V
D3
V
D3
T2
D3
Unit 1
Unit 2a
Unit 2b

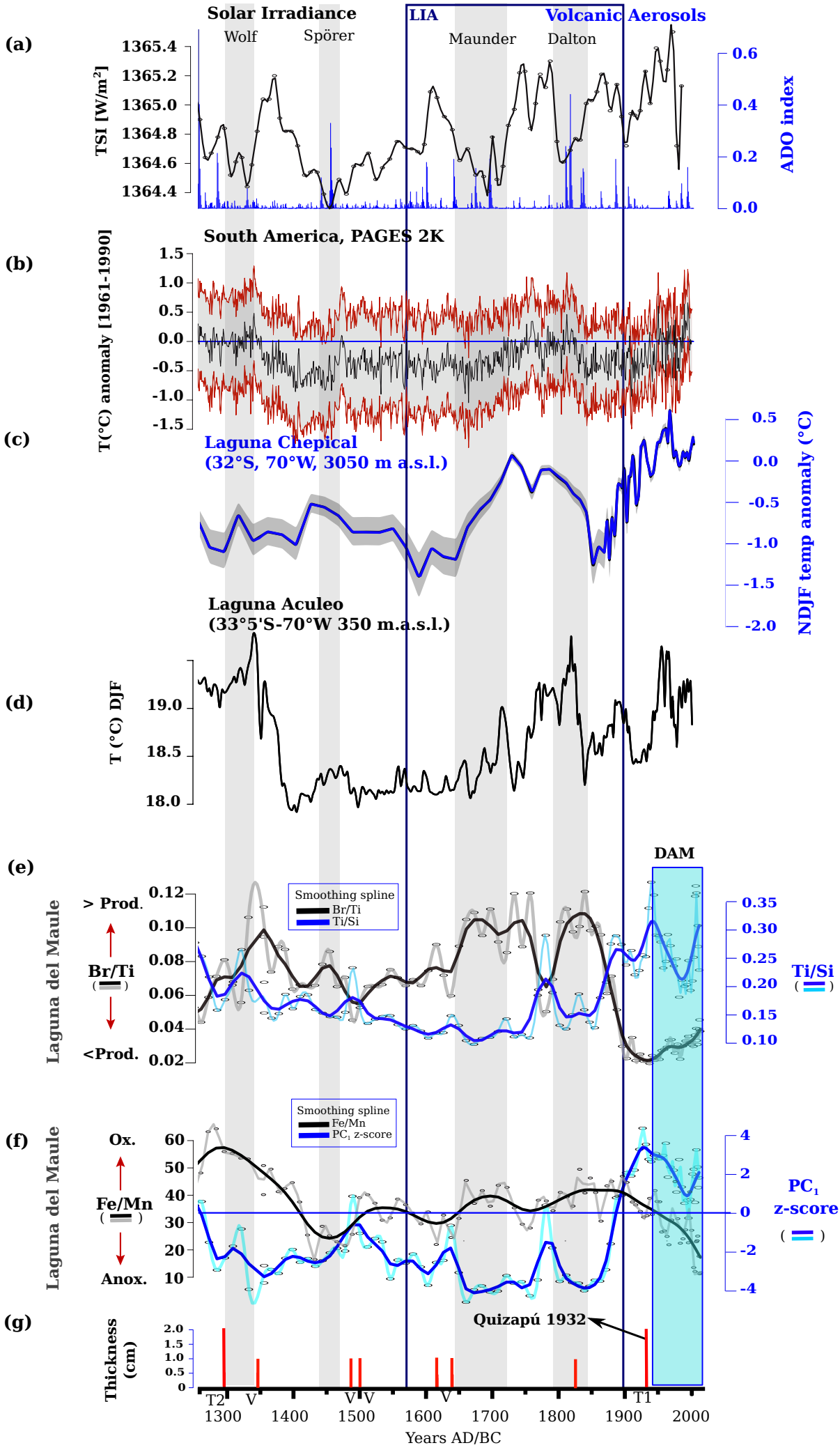
(a)
Solar Irradiance
Wolf
Spörer
LIA
Maunder
Dalton
Volcanic Aerosols
TSI [W/m²]
1365.4
1365.2
1365.0
1364.8
1364.6
1364.4
ADO index
0.6
0.4
0.2
0.0
(b)
South America, PAGES 2K
T(°C) anomaly [1961-1990]
1.5
1.0
0.5
0.0
-0.5
-1.0
-1.5
(c)
Laguna Chepical
(32°S, 70°W, 3050 m a.s.l.)
NDJF temp anomaly (°C)
0.5
0.0
-0.5
-1.0
-1.5
-2.0
Laguna Aculeo
(33°5'S-70°W 350 m.a.s.l.)
(d)
T (°C) DJF
19.0
18.5
18.0
(e)
DAM
Laguna del Maule
> Prod.
Br/Ti
<Prod.
Smoothing spline
Br/Ti
Ti/Si
0.12
0.10
0.08
0.06
0.04
0.02
0.35
0.30
0.25
0.20
0.15
0.10
Ti/Si
(f)
Laguna del Maule
Ox.
Fe/Mn
Anox.
Smoothing spline
Fe/Mn
PC₁ z-score
60
50
40
30
20
10
4
2
0
-2
-4
PC₁
z-score
(g)
Thickness (cm)
2.0
1.5
1.0
0.5
0
Quizapú 1932
T2
V
V
V
V
T1
1300
1400
1500
1600
1700
1800
1900
2000
Years AD/BC

Supplemental Files

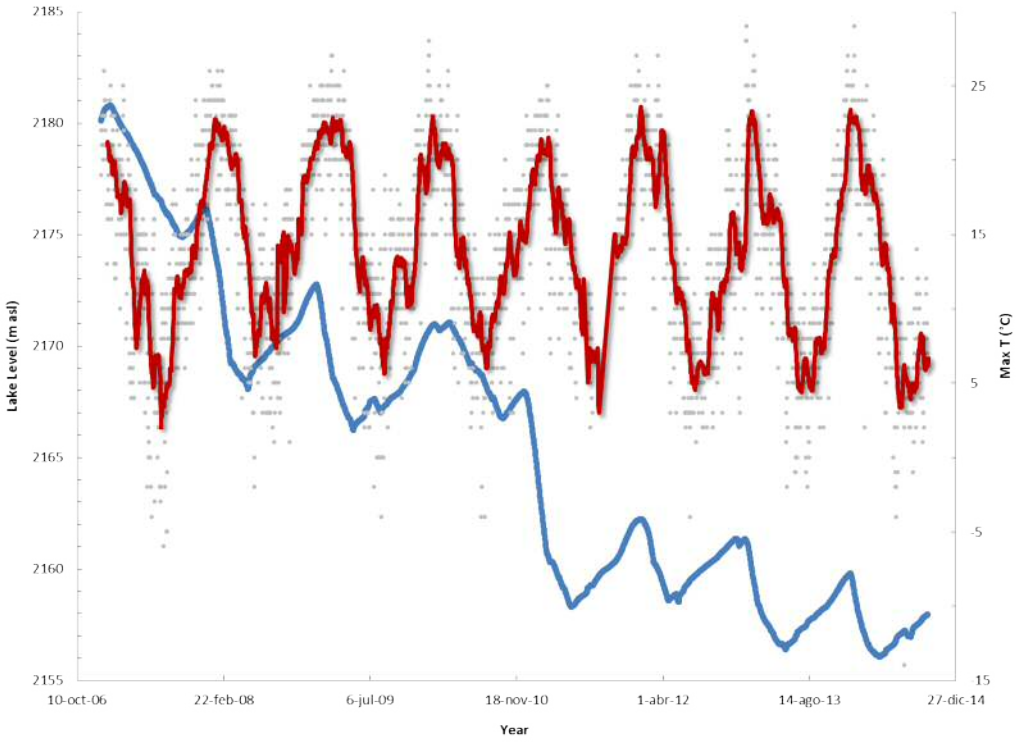

Figure 1. Lake levels (masl, in blue) and maximum daily temperatures (°C, gray dots with 23 yr moving average in red), for the past decade in LdM.

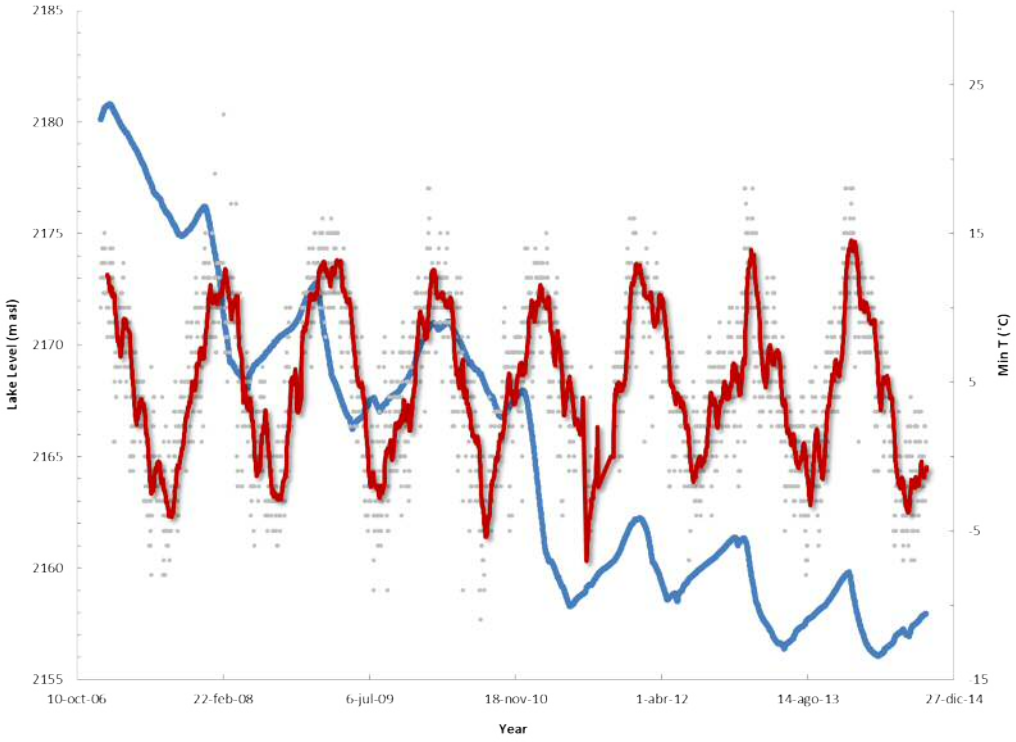

Figure 2. Lake levels (masl, in blue) and minimum daily temperatures (°C, gray dots with 23 yr moving average in red), for the past decade in LdM.

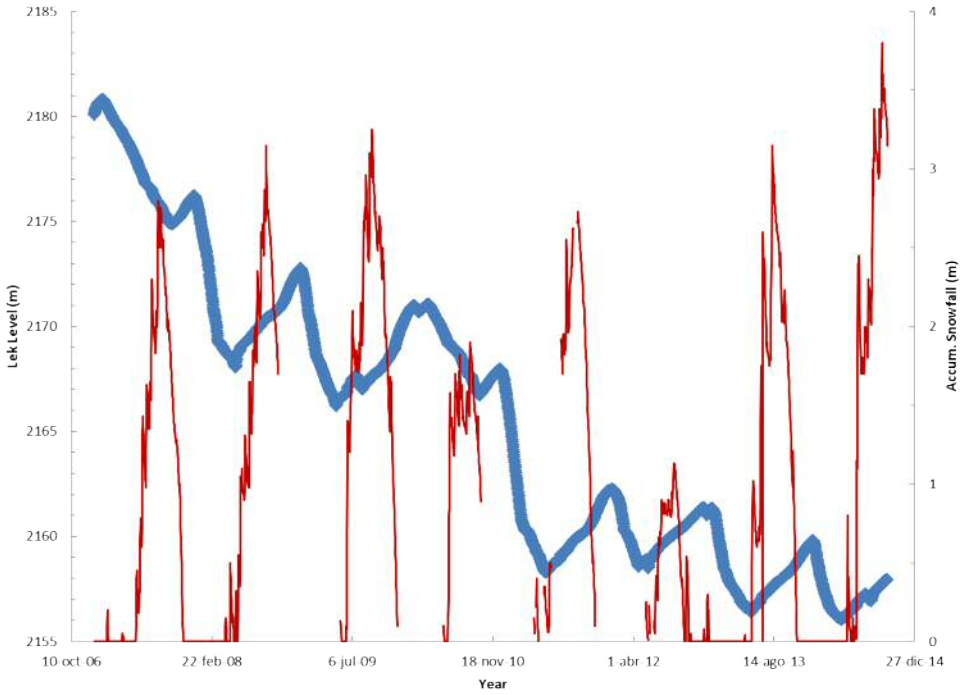

Figure 3. Lake levels (masl, in blue) and precipitations as accumulated snow (m, in red), for the past decade in LdM.

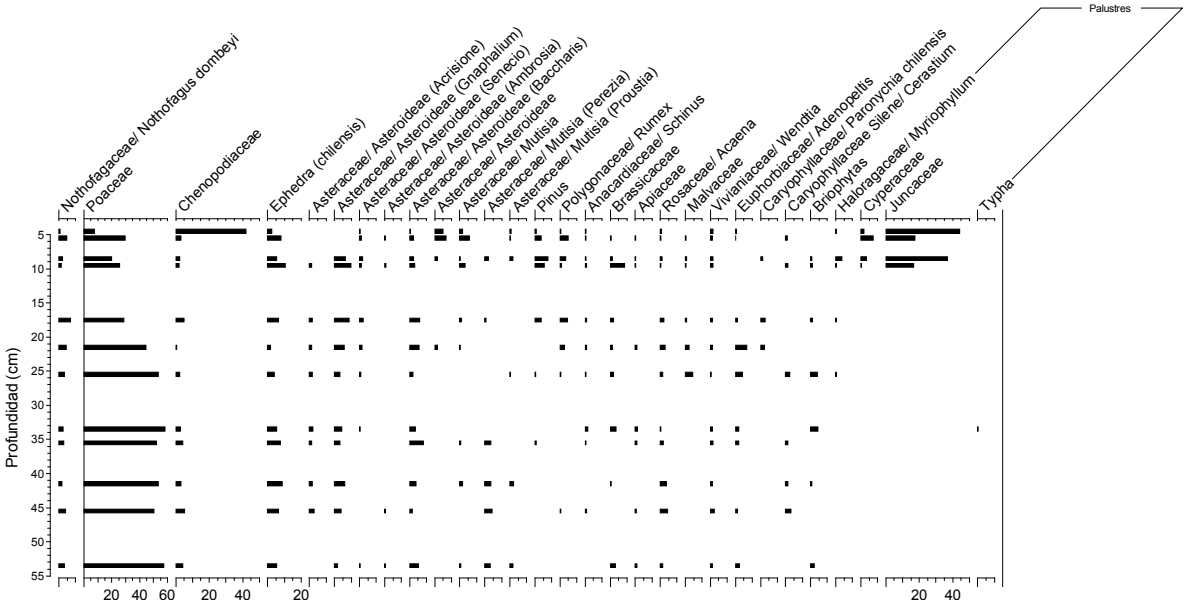

Figure 4. Pollen accumulation rates of LdM.

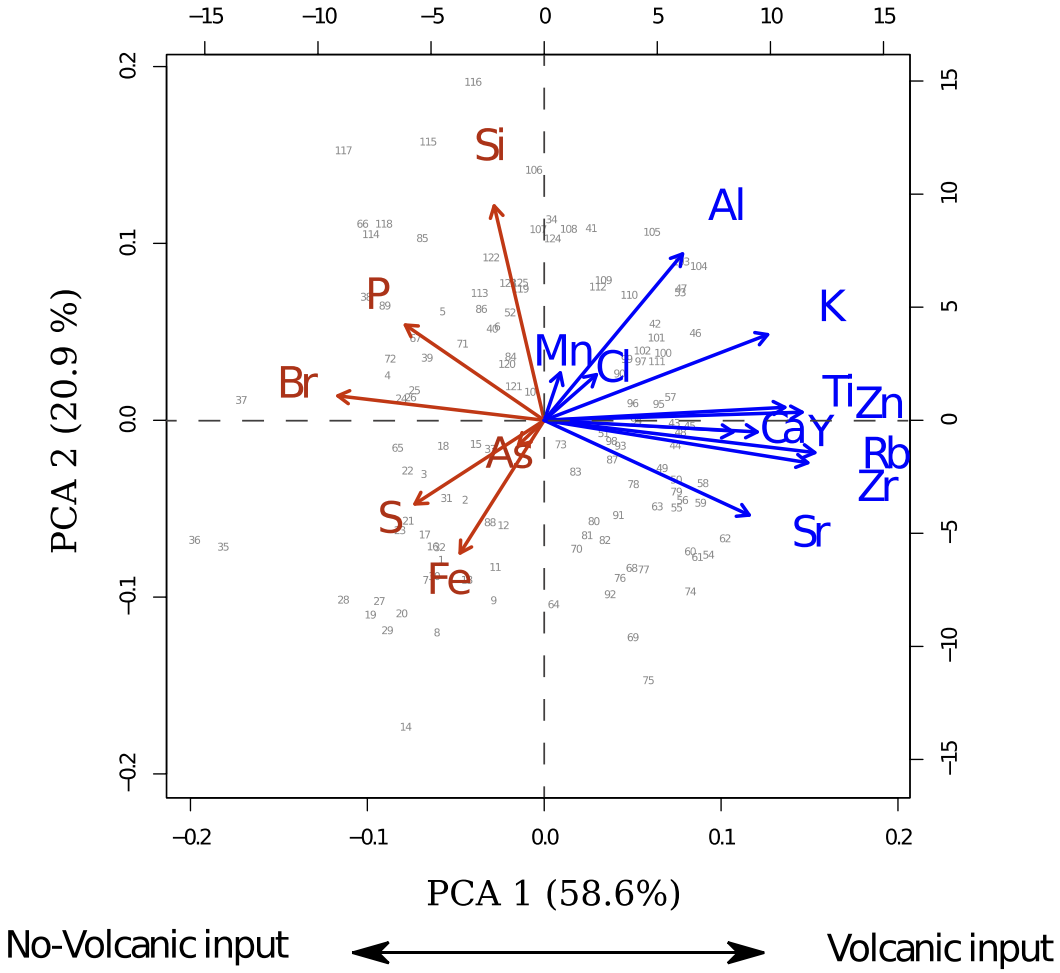

Figure 5. First two components of a PCA of the XRF core scanner dataset.

Table 1. Identification, latitude and longitude dates and analyses developed on the short cores reported here at Laguna del Maule.

ID Section Core	ID abbreviated	Latitude (UTM)	Longitude (UTM)	Length (cm)	Depth (m)	Analyses developed
LEMA-LEM11-1A-1G-1	LEM11-1A	6010779	360347	48	46	Sedimentological description, geochemical and biologic proxies, comparison of TOC, radiocarbon dates, correlation of T1 tephra
LEMA-LEM11-2A-1G-1	LEM11-2A	6011009	359828	22	58	Sedimentological description, comparison of TOC, correlation of T1 tephra
LEMA-LEM11-3A-1G-1	LEM11-3A	6010520	360903	79	24	Sedimentological description, comparison of TOC, correlation of T1 tephra, radiocarbon date
MAUEN-LEM12-1A-1G-1	LEM12-1A	6013809	368543	30	4.3	Sedimentological description, comparison of TOC, correlation of T1 tephra
MAUEN-LEM12-3A-1G-1	LEM12-3A	6010934	366586	21	48,5	Sedimentological description, comparison of TOC, correlation of T1 tephra, correlation with LEM12-3B
MAUEN-LEM12-3B-1G-1	LEM12-3B	6010934	366586	29	48.5	Sedimentological description, comparison of TOC, correlation of T1 tephra, $^{210}Pb/^{137}Cs$ dating
MAUEN-LEM12-4A-1G-1	LEM 12-4A	6006964	366212	25	31	Sedimentological description, comparison of TOC, correlation of T1 tephra
MAUEN-LEM13-3C-1G-1	LEM13-3C	6010066	365499	52	44	Sedimentological description, comparison of TOC
MAUEN-LEM13-3D-1G-1	LEM 13-3D	6010065	365498	49.7	44.5	Sedimentological description, comparison of TOC

Table 2. Zones or vegetation belts present in the study area	
Vegetation belts	
Dominant species	Type
High Andean Shrubland belt	
Berberis empetrifolia	shrubs
Laretia acaulis	shrubs
Oxalis compacta	Herbs and forbs
Poa holciformis	Herbs and forbs
Bromus setifolius	Herbs and forbs
Hordeum comosum	Herbs and forbs
Acaena pinnatifida	Other associated species -
Anarthrophyllum gayanum	"
Astragalus vesiculosus,	"
Azorella madreporica,	"
Azorella montana	"
Doniophyton weddellii	"
Glandularia microphylla	"
Junellia uniflora	"
Malesherbia mendocina,	"
Mutisia sinuata	"
Oreopoulus gracilis	"
Oxalis hypsophila	"
Perezia carthamoides	"
Phacelia secunda	"
Phleum alpinum	"
Senecio clarioneifolius	"
Senecio gilliesii	"
Senecio multicaulis	"
Tropaeoloum polyphyllum	"
High Andean Steppe (herbs and cushion species)	
Oxalis holoserica	Herbs and forbs
Oxalis adenophylla	Herbs and forbs
Discaria nana	Herbs and forbs
Plantago pauciflora	Herbs and forbs
Nassauvia lagascae	Herbs and forbs
Nassauvia revoluta	Herbs and forbs
Nassauvia pygmea	Herbs and forbs
Pozoa coriacea	Herbs and forbs
Schizanthus grahamii	Herbs and forbs
Viola sempervivum	Herbs and forbs
Pernettya pumila	Herbs and forbs
Low Andean Shrubland	
Chuquiraga oppositifolia	Shrubs
Discaria articulata	Shrubs
Baccharis neaei	Shrubs
Mulinum spinosum	Shrubs
Ephedra chilensis	Shrubs
Guindilla trinervis	"
Euphorbia collina	"
Schizanthus grahamii	Herbs and forbs
Oxalis polyantha	Herbs and forbs
Alstroemeria	Herbs and forbs
Loasa volubilis	Herbs and forbs
Monteopsis sericea	Herbs and forbs
Quinchamalium chilense	Herbs and forbs
Deciduous Forest	
Nothofagus obliqua	Trees

Table 3. *in situ* pH measurements of Laguna del Maule

	Site	Date	Hour	Coordinates	Reference	Zone	pH	H (altura)	Sigla	Photo	Sample collected
1	LdM	11-03-2013	16:54	36 0,965'S	Torre	DIATO COSTA	7,7		LEM13 1D	si	plankton
				70 33,448W+-3							benthos
											epilithon
											macrophytes
2	LdM	11-03-2013	18:38	36 01778'S	Bandera		7,3		LEM13 2D	si	
				70 55890'W							
				19H 0359527							
				6012955							
3	LdM	13-03-2013			Playa fondo Laguna	DIATO COSTA	8,4		LEM13 3D		plankton
4	LdM	13-03-2013		36 03,922'S	Agua		5,9	2199	LEM13 T1		plankton
				070 27594'W							benthos
											epilithon
											macrophytes
5	LdM	13-03-2013			Sondeo				LEM13 2C2U		
6	LdM	13-03-2013			Sondeo				LEM13 1B1U		
7	LdM	13-03-2013			Sondeo				LEM13 1A1U		
8	LdM	14-03-2013		36 02,256'S	Punto 10		7,0		LEM13 4D		plankton
				70 32,205'W							benthos
											epilithon
											macrophytes
9	LdM	14-03-2013							LEM13 5D		plankton

10	LdM	14-03-2013		19H X 0363114			6,1?				benthos
				19H Y 6012325							epiliton
											macrophytes
11	LdM	14-03-2013			Punto 07				LEM13		diatomite
11'	LdM	14-03-2013			Punto 19				LEM13		diatomite
12	LdM	14-03-2013							LEM13		diatomite (more pure)
13	LdM	14-03-2013		19H X 0363459			7,0		LEM13 6D		plankton
				19H Y 6012468 +-3m							benthos
											macrophytes
14	LdM	14-03-2013			Punto 11 Fuente1		7,3		LEM13		plankton
					Fuente1				LEM13		diatomite
15	LdM	16-03-2013							LEM13 3A 1U		plankton
16	LdM	16-03-2013							LEM13 3C 1G		plankton
17	LdM	16-03-2013		36 04272 S			7,0	2160	LEM13 7D		plankton (Seismic)
				070 49214 W							

Table 4. PCA of the XRF core scanner dataset of Laguna del Maule

Importance of components:				
	PC1	PC2	PC3	PC4
Standard deviation	2.7548	1.6476	1.2285	1.06145
Proportion of Variance	0.5865	0.2098	0.1166	0.08707
Eigenvalues				
	7.588693	2.71474	1.50915	1.126668
Loadings				
	PC1	PC2	PC3	PC4
Al	0.18398866	0.434006776	-0.1194926	0.155656107
Si	-0.04907239	0.5837604	-0.35387965	0.130364395
P	-0.1941357	0.388037119	-0.2448284	-0.422405911
S	-0.15913256	-0.355333745	-0.70666338	0.213273172

Cl	0.08892799	0.029529607	0.09990946	0.002818363
K	0.29039685	0.197245308	-0.11481629	0.040437733
Ca	0.27450379	-0.018331928	-0.25857923	-0.00306934
Ti	0.32166295	0.05823895	-0.11383619	-0.011057962
Mn	0.02502962	0.192962668	0.16644929	-0.310581042
Fe	-0.0447788	-0.183636531	-0.30387861	-0.732535662
Zn	0.34193216	0.059765794	0.04072104	-0.056149233
As	-0.07335565	-0.042048649	0.194832	-0.19470845
Br	-0.29908615	-0.002415527	-0.10958238	0.22809969
Rb	0.34847836	-0.101527864	-0.04108382	-0.009365548
Sr	0.29891437	-0.225234127	-0.15497895	-0.047629005
Y	0.29410333	-0.004089262	-0.01983204	-0.064697486
Zr	0.3435168	-0.114732783	-0.02041543	0.019610792